

NATIONAL TRANSPORTATION SAFETY BOARD

Office of Research and Engineering
Materials Laboratory Division
Washington, D.C. 20594



April 24, 2006

MATERIALS LABORATORY FACTUAL REPORT

Report No. 06-010

A. ACCIDENT

Place : Miami, Florida
Date : December 19, 2005
Vehicle : Grumman G-73T Mallard, N2969
NTSB No. : DCA06MA010
Investigator : Brian Murphy, AS-40

B. COMPONENTS EXAMINED

Pieces of the wing box beam.

C. DETAILS OF THE EXAMINATION

A schematic view of the right side of the wing box beam for the Grumman model G-73 (Mallard) airplane is shown in figure 1. The wing box beam is located between right wing station (WS) 125¹ and left WS 125 and is positioned near the wing leading edge. The wing box beam incorporates the carrythrough structure of the wings. The fuselage wall intersects the aft side of the wing box beam at right and left WS 34. Portions of the wing box beam also serve as fuel tanks as shown in figure 1. The wing box beam was not changed when the model G-73 was converted to a model G-73T.

The wing box beam for the Grumman model G-73 has spars at the forward and aft sides and skin panels at the upper and lower sides. The upper skin panel has three hat-shaped stringers, and the lower skin panel has three Z-shaped stringers. Ribs for the wing box beam are located at the centerline and right and left WS 13, 26, 34, 48, 62, 77, 92, 107, and 125. Received pieces of the wing box beam included portions of the rear spar, forward spar, skin, stringers, and ribs from various areas on both the left and right sides.

The right wing separated from the remainder of the airplane approximately at right WS 34. Pieces were received by the Safety Board's Materials Laboratory in stages. Pieces from the inboard end of the right wing portion of the wing box beam that separated from the airplane in flight plus two pieces of the rear spar lower spar cap were first to arrive. Next, pieces of the rear spar lower spar cap, rib, and lower skin panel at left WS 34 arrived.

¹ Wing station numbers correspond to the distance in inches outboard from the airplane centerline.

Finally, other pieces including pieces from the carrythrough portion of the wing box beam were received.

All fracture surfaces of the submitted pieces from the wing box beam were examined visually. Most of the fractures had deformation, fracture surface roughness, and slant angle fractures consistent with overstress fracture. However, between right and left WS 62, some fractures of the lower skin, Z-stringers, and lower spar caps had features indicative of preexisting cracking or fracture. These areas of structure were examined in greater detail as described below. To facilitate the examination, repair doublers and internal stiffeners located near right and left WS 34 were removed from the lower skin. Photographs and visual observations of the parts as received and both during and after the doubler removal process are presented in the next section. Photographs and details of the fracture surfaces are presented in the subsequent section titled "Fractographic Examination."

Visual Examination and Repair Doubler Removal

Adjacent to Right WS 34

The pieces from the wing box beam that were first to arrive in the Safety Board's Materials Laboratory are shown in the overall view in figure 2. The pieces shown in figure 2 are primarily from the inboard end of the portion of the wing box beam that remained with the right wing. Two pieces of the rear spar lower spar cap from the main portion of the airplane were also in the first group of pieces to arrive. The fracture occurred mostly within the fuel tank just outboard of right WS 34, and the interior of the submitted pieces outboard of the fracture were coated with sealant. The pieces of the wing box beam had been cut approximately 2 to 3.5 feet from the fracture location to facilitate shipping to the Safety Board's Materials Laboratory.

The lower skin panel of the wing box beam contained an external repair doubler and a series of internal repair doublers adjacent to the right WS 34 fracture. The lower skin fracture was mostly recessed between these doublers. Views of the external doubler on the lower surface of the wing box beam adjacent to right WS 34 are shown in figures 3 and 4. Some sooting was present on the lower surface of the lower skin panel piece. The area with the repair doubler was not sooted. On the Grumman model G-73 (and G-73T) airplane, the area with the repair doubler is not visible on the exterior of the airplane since it is covered by a fairing between the wing and the fuselage. A fuel sump drain is also located in the area covered by a fairing as indicated in figure 4.

To facilitate handling of the repair area in the lower skin panel, the aft piece of the lower skin panel shown in figures 3 and 4 was cut chordwise just outboard of the external repair doubler. To separate the doublers from the skin panel, rivets in the area of the repair doubler shown in figure 4 were removed using two methods. For the rivets with protruding heads, the heads of the rivets were sheared off using a chisel and hammer. The remaining rivets with flush heads were removed by drilling out the centers of the rivets using a countersink drill bit until the heads were separated from the shank. Additionally, the sump drain fitting was removed by unscrewing it from the sump drain reinforcement plate. The

doubler was then pried from the skin using wooden tongue depressors. The faying surfaces between the skin and external doubler after separation are shown in figure 5. The skin fracture is at the top edge of the piece as it is oriented in this figure.

A crack was observed in the skin in the area that had been covered by the external doubler. A closer view of the crack in the lower skin is shown in figure 6. The crack was oriented chordwise, approximately parallel to the skin fracture, and was 15.9 inches long. The aft end of the crack intersected the skin trailing edge, and the skin fracture intersected portions of the crack near the rear spar. The forward end of the crack was located at the aft side of the middle Z-stringer lower flange. The crack also intersected an area of hard green sealant around the sump drain and fastener holes for two rib stiffeners and for the rear Z-stiffener. The crack intersected three unfilled machined holes in the skin that were not in line with fasteners for internal stiffeners and did not have corresponding holes in the doublers, features consistent with stop drill holes. The locations of the stop drill holes were 8.8 inches, 6.9 inches, 15.9 inches forward of the skin trailing edge. The hole at 15.9 inches forward of the skin trailing edge corresponded to the forward end of the crack, and the hole also extended through the edge of the Z-stringer lower flange.

The crack could be considered as two segments consisting of an aft segment that intersected the green sealant around the fuel sump drain and a forward segment that intersected fasteners for the rib stiffeners and the rear Z-stringer. The forward segment of the crack was located slightly outboard of the aft segment of the crack, and the crack segments intersected each other at two locations near the rearmost rib stiffener. The aft end of the forward crack segment intersected the aft crack segment just aft of the rearmost rib stiffener at a feature labeled as a divot in figure 6. The divot was a machined, spherical section of missing material consistent with a partially-drilled hole. The forward end of the aft segment of the crack intersected the forward segment of the crack just forward of the rearmost rib stiffener.

A closer view of the crack in the vicinity of the fuel sump drain hole is shown in figure 7. Skin was mostly missing from the area between the fuel sump drain hole and the ring of fasteners around the hole, and the hard green sealant was observed in its place. Also visible in figure 7, the lower surface of the rear spar was roughened and darkened consistent with corrosion.

Next, the three internal doublers were removed from the skin. The fasteners that had their heads sheared off during the external doubler removal were pushed inward using a punch and hammer. Also, the fuel tank sealant was cut with a knife around the edges of the internal doubler. Then the internal doublers were pried off using wooden tongue depressors.

An overall view of the pieces after removing the doublers and stiffeners from the skin is shown in figure 8. Faying surfaces of the doublers and Z-stringers and the upper skin surface are shown. To facilitate examination of the skin crack, the skin was cut from the fracture surface outboard to the forwardmost stop drill hole, and the skin is shown in figure 8 with that cut made.

A closer view of the faying surface on the upper side of the skin near the middle Z-stringer is shown in figure 9. The photo shows the area before the cut was made to separate the crack surfaces. The skin faying surfaces for the internal doublers appeared relatively shiny and had a somewhat random scrape pattern. In one area adjacent to the faying surface of the rib stiffener shown in figure 10, material had been removed in a circular area that contained a curved pattern of scratches, identified as a whirl in figure 10. Sealant from this whirl area remained attached to one of the internal doublers, and this sealant retained the shape and scratch pattern from the whirl cavity.

In removing the internal doublers, it was noted that most of the areas of sealant consisted of multiple layers. In one area at the edge of an internal doubler where the sealant was 0.37 inch thick, seven layers were observed. From the internal doubler surface upward, the layers were a light gray layer, a dark gray layer, a relatively thinner tan layer, a medium gray layer, a dark gray layer, a light gray layer, and at the inner surface a relatively thinner red layer.

The rear spar lower spar cap adjacent to the fracture just inboard of right WS 34 is shown in figure 11. Sealant was removed from the area by cutting with a razor, soaking with toluene, and scraping with wood or plastic instruments. Grinding or sanding marks were observed on the upper surface of the horizontal flange. Corrosion pits were also observed, particularly around the washers for the threaded fasteners.

At Left WS 34

An overall view of the first pieces received in the Safety Board's Materials Laboratory from the left wing side of the wing box beam is shown in figure 12. The pieces included portions of the lower skin panel, the left WS 34 rib, and the rear spar lower spar cap, all from an area near the lower aft side of the wing box beam spanning across left WS 34. Internal and external repair doublers were attached to the skin panel.

The pieces comprised part of the inboard end of the left wing fuel tank, and the internal surfaces outboard of left WS 34 were covered with sealant as shown in figure 12. On the larger piece shown in figure 12, the lower skin panel was fractured at the inboard, outboard, and forward sides of the piece. (The aft edge of the skin panel is a manufactured edge.) The rear spar lower spar cap piece (smaller piece in figure 12) had a fracture surface at its inboard end and a cut surface at its outboard end.

The external doubler on the lower surface of the larger piece from figure 12 is shown in figure 13. The skin fracture occurred mostly within the boundary defined by the edge of the external doubler, and no skin is visible in figure 13. The horizontal flange of a portion of the fuselage attachment angle was attached to the piece as shown in figure 13. The fuselage attachment angle was fractured in the transition radius between the horizontal and vertical flanges of the angle. The lower surface of the external doubler was rough and pitted around the fuel sump drain consistent with corrosion in that area.

The heads of most of the fasteners at the lower surface shown in figure 13 were flush to the surface. These fasteners were removed by drilling with a countersink drill bit through the rivet centers. Fasteners around the fuel sump drain had protruding heads, and those fasteners were removed by shearing the heads using a chisel and hammer. As these fasteners were removed, pieces of the external doubler that were thinned down from corrosion broke off around the fuel sump drain hole. Threaded fasteners for the fuselage attachment angle and adjacent to the angle were removed by unscrewing the nut and then pulling and/or pushing the bolt out of its hole. The fuel sump drain also was unscrewed from the reinforcement plate. The external doubler was removed by prying it from the skin using wooden tongue depressors.

The faying surfaces between the skin and the external doubler are shown in figure 14 after the external doubler was removed. A repair filler piece in the skin as indicated in figure 14 was observed within the area of skin covered by the external doubler. Some corrosion was observed on the faying surface of the lower skin in the area of the fuselage attachment angle holes. Also visible in figure 14 is the irregularly-shaped hole in the doubler material around the sump drain where material substantially thinned by corrosion had broken away during rivet removal.

Some flush head fasteners were present fastening the skin and the internal doublers. These fasteners were removed by drilling through the fasteners with a countersink drill bit. Then, the internal doublers and rib attach angle pieces were pried from the skin and repair filler pieces using wooden tongue depressors. An overall view of the skin and the faying surfaces of the pieces that were attached to it is shown in figure 15.

Many open holes filled with sealant were present in the lower skin panel within the area covered by the external doubler. The open holes generally had a diameter that was slightly smaller than the filled holes. Lines of open fastener holes in the lower skin are indicated in figure 14. Two open holes were also present in the repair filler piece. Open holes filled with sealant were also observed in the internal doublers at locations corresponding to the open holes in the skin and repair filler.

Severe corrosion was observed in the lower skin just inboard of the filler piece. The skin was pitted and substantially thinned in areas near the fuselage attachment angle holes.

As shown in figure 16, the rear spar lower spar cap was thinned in an area just inboard of left WS 34. Grinding or sanding marks were observed on the upper surface of the horizontal flange, and several rivet tails were missing. Corrosion pits were also observed, particularly around holes for bolted fasteners.

Fractographic Examination

Additional pieces from the wing box beam were received by the Safety Board's Materials Laboratory after doublers had been removed from the previously submitted skin pieces at left and right WS 34. The overall photos in this section of the report show the

additional pieces as received and the pieces from the repair areas with the doublers removed.

Wing Carrythrough

An overall view of the recovered pieces from the lower side of the wing box beam in the carrythrough portion between left and right WS 34 is shown in figure 17. These pieces mostly remained with the main portion of the airplane after separation of the right wing. The lower spar caps for the front and rear spars and the skin panel were fractured chordwise near the centerline. The skin panels also were fractured spanwise in several locations. The chordwise fractures near the centerline and the spanwise fractures in the skin panels showed deformation, rough fracture surfaces, and slant fracture planes consistent with overstress fracture. Other fractures on these pieces near right and left WS 34 will be discussed subsequent sections of this report.

The lower surface of a piece of the lower skin at and inboard of right WS 34 is shown in figure 18. The piece of skin included fastener holes for the fuselage attachment angle attachment bolts. One of the holes as indicated in figure 18 had a double-drilled opening.

Right Wing near WS 34

A diagram showing the approximate locations of fractures and the skin crack in the area of the repair near right WS 34 is shown in figure 19. Some of the structural features in the area are also shown, including the repair doublers, Z-stringers, rear spar lower spar cap, rib, and fuselage attachment angle.

An overall view of the lower skin panel and lower spar cap pieces from the wing box beam at right WS 34 are shown in figure 20. The pieces in this figure are arranged approximately in the same orientation as the diagram in figure 19. Unlabeled arrows and brackets in figure 20 indicate locations in the rear spar lower spar cap, rear Z-stringer, and lower skin where features typical of fatigue were observed on the fracture surfaces. These areas will be individually discussed in the following sections.

Rear Spar Lower Spar Cap

The rear spar lower spar cap had a transverse fracture approximately one inch inboard of right WS 34 that intersected the outboard bolt hole for the horizontal flange of the fuselage attachment angle as shown in the drawing in figure 19. A secondary fracture intersected the transverse fracture and the inboard bolt hole for the horizontal flange of the fuselage attachment angle, and the piece of spar cap between the two fractures was missing.

Views of the outboard surface of the transverse fracture in the rear spar lower spar cap are shown in figures 21 and 22. Portions of the fracture surface appeared relatively flat with smoothly curving arrest lines, features consistent with fatigue. A closer view of the

fatigue region in the horizontal flange of the spar cap is shown in figure 23, where dashed lines indicate the fatigue boundaries. Fatigue features emanated from the bolt hole for the outboard fastener for the fuselage attachment angle. Multiple fatigue origins were observed along the hole bore through the thickness within the regions defined by the unlabeled brackets in figure 23. A closer view of the bolt hole and fatigue origin area is shown in figure 24.

Relatively flat regions with large numbers of crack arrest positions, indicative of slower growth fatigue cracking, emanated from the origin areas both forward and aft of the bolt holes. These slower growth regions extended a maximum of 0.15 inch forward of the bolt hole and 0.07 inch aft of the bolt hole, up to the positions indicated by the dashed lines in figure 24. The remainder of the fatigue region beyond the dashed line positions in figure 24 had a mixture of curving flat regions with crack arrest positions (appearing light gray in figures 23 and 24) separated by rougher regions without crack arrest positions (appearing darker gray in figures 23 and 24). The flat light gray regions indicate areas of relatively slow crack growth and crack arrest, and the rougher, darker gray regions indicate areas of relatively fast crack growth or overstress regions. Upon inspection under magnification, approximately 11 areas of relatively slow growth between areas of fast growth were observed in the fatigue region aft of the bolt hole.

As indicated by the two white arrows in figure 22, the bolt hole consisted of two separately drilled channels. One of these channels had an axis perpendicular to the flange surface, and the other channel had an axis at an angle of approximately 17 degrees from perpendicular, with the lower end of the hole being further aft than the upper end of the hole. Corrosion and deposits were greater in the portion of the hole corresponding only to the perpendicular channel, suggesting that the fuselage attachment angle bolt had last been installed through the angled channel.

To facilitate an examination of the fatigue fracture surface using scanning electron microscopy (SEM), the rear spar lower spar cap was sectioned with a transverse cut approximately $\frac{3}{4}$ inch outboard of the fracture surface. The piece was then cleaned in a soap water solution with an ultrasonic cleaner followed by an alcohol rinse.

An SEM view of the origin area at the aft side of the bolt hole after cleaning is shown in figure 25. Several main origin areas were observed separated by ratchet marks² as indicated by unlabeled brackets in figure 25. Unlabeled arrows in figure 25 indicate general directions of fatigue propagation as evidenced by crack arrest lines.

A higher-magnification view of typical fracture features near the origin areas is shown in figure 26. Fine fracture features were obliterated by corrosion and rubbing, but generally the features appeared relatively smooth and flat.

² A ratchet mark is a small step in the fracture surface formed when two adjacent fatigue cracks originate on slightly offset planes.

A higher-magnification view of fracture features in a relatively slow growth region near the boundary at the aft end of the fatigue region is shown in figure 27. Fine fracture features were obliterated by corrosion, but some faint curving parallel lines such as the one indicated in figure 27 were observed in a few locations near the boundary.

A piece of the rear spar lower spar cap inboard of right WS 34 was also recovered. This piece contained the aft portion of the mating inboard surface of the transverse fracture just inboard of right WS 34. However, this side of the fracture was not examined in detail. The forward side of the bolt hole and mating fracture surface at the origin areas were missing from that piece.

Rear Z-stringer

The rear Z-stringer had a transverse fracture located 1.5 inches outboard of right WS 34. An overall view of the outboard side of the fracture is shown in figure 28 as received before separating the stringers and doublers from the skin. The fracture in the Z-stringer intersected a slosh hole in the center of the web of the stringer as indicated in figure 28. Portions of the fracture were relatively flat and on a perpendicular plane to the length of the stringer, features consistent with fatigue. These flat regions also had curving boundaries and arrest lines, further indications of fatigue. Fatigue features emanated from the slosh hole area as indicated with unlabeled arrows in figure 28. Portions of the fracture surface shown in figure 28 were covered with sealant, and features from the mating fracture surface were observed on the sealant surface.

After disassembly of the stringer piece from other structure, sealant was removed from the fracture surface on the Z-stringer and from the stringer surfaces adjacent to the fracture surface. For sealant on the fracture surface, the sealant was cut with a knife around the edges of the fracture and the sealant was pulled from the surface where possible. Additionally, sealant and debris was removed using replica tape. On the surfaces adjacent to the fracture surface, sealant was removed by cutting around the area to be removed with a knife, pulling with pliers, and scraping with wood or plastic instruments. A view of the fractured end of the Z-stringer piece after sealant removal is shown in figure 29. As indicated in figure 29, grinding or sanding marks were observed in the area of the slosh hole. Also, the web was thinned around the forward edge of the hole, particularly around the upper side of the hole where the thinning tapered the edge of the hole to a point near the aft side of the web.

Close views of the outboard fracture surfaces on the upper and lower side of the slosh hole in the rear Z-stringer are shown in figures 30 and 31. On the upper side of the slosh hole, fatigue features emanated upward as indicated by the unlabeled arrow to the boundary indicated by a dashed line. Most of the upper flange for the Z-stringer was fractured on a slant plane consistent with overstress fracture. However, the fracture surface was relatively smooth, consistent with rubbing and wear contact with the mating fracture surface over some period of time.

At the lower side of the slosh hole for the rear Z-stringer, fatigue features emanated downward through the web and aft through the lower flange as indicated with unlabeled arrows in figure 31. Fatigue features in the lower flange emanated aft as far as within 0.04 inch of the aft side of the flange.

The rear Z-stringer was cut approximately one inch outboard of the fracture surface, cleaned in an ultrasonic cleaner with soap water, and then rinsed with alcohol to facilitate an examination of the fracture surface using SEM. Figures 32 and 33 show the fracture surface at the upper and lower sides of the slosh hole as viewed using SEM. At the upper side of the slosh hole as shown in figure 32, a ratchet mark was observed, indicative of multiple fatigue origins. However, specific origin areas were not apparent. Lips of deformed material were present at the edges of the fracture surface in areas including the origin areas as shown in figure 32. The deformation lips appeared to be associated with grinding or sanding marks in the Z-stringer web. The deformation lips were rolled onto the fracture surface consistent with deformation lips occurring after the Z-stringer was cracked in the lipped area. A review of early photos taken before sealant was scraped away also showed the presence of deformation lips on the fracture surface.

As shown in figure 33, deformation lips were also observed around the edges of the fracture surface at the lower side of the slosh hole. Fracture features showed an origin generally located at the surface of the slosh hole, but no specific origin location was apparent. Deformation lips were present in the general origin area and were lipped onto the fracture surface consistent with post-fracture damage, similar to the deformation lips found on the upper side of the slosh hole.

The mating inboard side of the fracture near right WS 34 in the rear Z-stringer was recovered in a piece of stringer that was 8.5 inches long. The piece is shown in the overall view of the pieces in figure 20. The mating side of the fracture had similar fracture features. In the overstress region through the upper flange, tan colored sealant was observed on the inboard side of the fracture surface.

Middle and Front Z-stringers and Front Spar Lower Spar Cap

The middle Z-stringer had a transverse fracture at 1.5 inches inboard of right WS 34. The fracture was relatively rough and on slant angles, features consistent with overstress fracture. The outboard side of the fracture was recovered on a piece of the Z-stringer that was attached to the aft piece of the lower skin panel, and the stringer piece was subsequently removed during the repair doubler removal process (see figure 8). This recovered piece of stringer also included the slosh hole in the center of the stringer web at 1.5 inches outboard of right WS 34. Sealant in the area of the slosh hole was cut, pulled, and scraped from the area, and a view of the hole is shown in figure 34. No cracks were observed at the hole when viewed using an optical stereomicroscope. Small areas of tool marks and missing material were observed as indicated with an unlabeled arrow in figure 34.

The forward Z-stringer had a transverse fracture located two inches inboard of right WS 34. Fracture features were relatively rough and were on slant planes, features consistent with overstress fracture.

The forward spar lower spar cap had a transverse fracture located one inch inboard of right WS 34. Fracture features were relatively rough and were on slant planes, features consistent with overstress fracture. Corrosion and loss of thickness was observed on the horizontal flange of the spar cap, particularly around threaded fasteners. Other areas of corrosion were covered with a light green paint.

Lower Skin

As shown schematically in figure 19, the skin was fractured chordwise, intersecting the fasteners at the inboard edge of the repair doublers. As previously discussed, the doublers covered a chordwise crack in the skin just outboard of the fracture. Portions of the fracture and the crack had flat features perpendicular to the skin surface with curving boundaries, features consistent with fatigue. On the airplane, all of the fatigue regions in the skin fracture and the crack just outboard of the fracture were covered on the inside by the internal stiffeners or the internal doublers and on the outside by the external doubler.

The fracture surfaces of the crack were partly covered with black sealant. Most of the sealant was removed on the inboard side of the crack surface by brushing the surfaces with a soft bristle brush and soapy water. After cleaning, the crack surfaces were examined using an optical stereomicroscope.

Results of the examination of the crack surfaces are shown in table 1. The segment of the skin crack that was closer to right WS 34 (the segment in the aft 6.1 inches) had features that emanated forward and aft from the area of green sealant around the fuel sump drain. As shown in table I, portions of this segment of crack had fatigue features, and portions had overstress features. In the length of crack from 1.1 to 3.3 inch from the aft edge, the crack was located at the edge of the green sealant or was through the sealant, intersecting the fuel drain hole and fasteners around the hole. This area of sealant, shown in light green around the fuel drain hole in figure 19, was translucent when focused light was applied to one side, indicating that no skin material was present in that area.

The segment of the skin crack that was further from right WS 34 (the forward segment) had features that emanated forward and aft from a fastener hole for the rear Z-stringer. The portion of the segment that emanated aft mostly in fatigue intersected a fastener hole for a rib stiffener and then turned to intersect the aft crack segment. The portion of the segment that emanated forward from the rear Z-stringer fastener hole had fatigue and overstress features and intersected three stop drill holes and a rib stiffener fastener hole.

Table 1. Crack Fracture Features

Distance from Aft Edge (inches)	Fracture Features Consistent with:	Crack Observations
0 – 0.5	Overstress	Slant angle
0.5 – 0.65	Fatigue	Relatively rough, but arrest lines visible, emanating aft
0.65 – 0.9	Fatigue	Flat fracture, emanating aft from origin at fastener hole
0.9 – 1.1	Fastener hole	Rear spar lower spar cap fastener
1.1 – 3.3		Crack adjacent to or through sealant, intersects fuel sump drain hole and surrounding fasteners
3.3-3.4	Fastener hole	Fuel sump drain plate fastener
3.4 – 3.7	Overstress	Irregular slant angle fracture
3.7 – 5.0	Fatigue	Flat fracture, rubbed with no clear arrest marks
5.0 – 5.6	Overstress	Slant angle, intersects divot
5.6 – 6.1	Fatigue	Flat fracture, arrest marks emanating forward
6.1		Abrupt step, intersect other crack segment
6.1 - 7.35	Fatigue	Flat fracture emanating aft from fastener hole for rear Z-stringer
7.35 - 7.45	Fastener hole	Rear Z-stringer fastener
7.45 - 8.75	Fatigue	Flat fracture emanating forward from fastener hole for rear Z-stringer
8.75 – 8.85	Hole	Stop drill
8.85 - 9.5	Overstress	Slant angle
9.5 - 10.1	Fatigue	Flat fracture, arrest marks emanating forward
10.05 - 10.2	Damaged	Post fracture damage
10.2 - 10.3	Hole	Stop drill
10.3 - 10.4	Fatigue	Flat fracture, arrest marks emanating forward
10.4 - 13.7	Overstress	Slant angle
13.7	Overstress	Abrupt step to intersect fastener hole
13.7 - 13.8	Fastener hole	Rib stiffener
13.8 - 15.8	Overstress	Slant angle
15.8 - 15.9	Hole	Stop drill hole at edge of Z-stiffener flange

An overall view of the skin fracture with doublers and stiffeners removed is shown in figure 35. As previously mentioned, the skin fracture followed the previous crack over portions of the aft segment of the crack. The crack and fracture paths coincided in two portions; 1) between the trailing edge and 0.63 inch from the trailing edge and 2) between 1.5 inches and 3.25 inches forward of the trailing edge where the crack and fracture both followed the edge of the hard green sealant. In the length of the fracture between 0.63 inch and 1.5 inches from the leading edge, the fracture intersected two rear spar lower spar cap fastener holes inboard of the crack.

Fastener holes intersected by the skin fracture forward of the green sealant were numbered for reference as shown in figure 35. On the skin fracture surface, fatigue features (flat regions with curving boundaries in planes perpendicular to the skin surface) were observed emanating from six of the fastener holes, four of which had fatigue regions on both the aft and forward sides of the hole. The fatigue regions locations and sizes are listed in table 2.

Table 2. Fatigue Regions Locations and Sizes in Skin Fracture

Fastener Hole Number	Distance from Trailing Edge (inch)	Width of Hole at Fracture Plane (inch)	Maximum Length from Fastener Hole Bore to Fatigue Boundary (inch)	
			Aft Side of Hole	Forward Side of Hole
1	3.75	0.15	0.008	0.010
2	4.63	0.14	0.025	0.038
5	6.5	0.18	0.107	0.070
6	7.31	0.11	Overstress	0.029
7	8.38	0.15	0.060	0.074
9	10.06	0.1	Overstress	0.016

Areas of the faying surface for the external doubler adjacent to right WS 34 are shown in figures 36 and 37. Fastener holes 4, 5, and 6 are indicated in figures 36 and 37, where the hole numbers correspond to the reference numbers for the skin as labeled in figure 35. At a location corresponding to the skin fracture, sealant on the fracture surface was lipped up as indicated with unlabeled arrows in figure 36. Inboard of the fracture location, sliding contact marks were observed and sealant was missing, as indicated with an unlabeled bracket in figure 36. Unlabeled arrows in figure 37 indicate a step in the surface of the doubler at the fracture location and spanwise sliding contact marks just inboard of the step, consistent with relative motion for some time between the external doubler and the fractured skin inboard of the fracture.

Left Wing near WS 34

A diagram showing the approximate locations of fractures in the area of the repair at left WS 34 is shown in figure 38. Some of the structural features in the area are also shown, including the repair doublers, Z-stringers, rear spar lower spar cap, rib, and fuselage attachment angle.

An overall view of the pieces from the lower portion of the wing box beam at left WS 34 are shown in figure 39. The unlabeled arrows and bracket in figure 39 indicate locations in the rear and middle Z-stringers, forward spar lower spar cap, and lower skin where features typical of fatigue were observed on the fracture surfaces. These fractures and other fractures in major structural elements from the lower portion of the wing box beam in this area are discussed in the following sections.

Rear Spar Lower Spar Cap

The rear spar lower spar cap had an approximately transverse fracture 6.5 to 7.25 inches inboard of left WS 34. The fracture was relatively rough and had slant angles, features consistent with overstress fracture.

Rear Z-stringer

The rear Z-stringer had a transverse fracture located 1 inch outboard of the left WS 34 and another fracture with transverse and longitudinal components between 0 and 1 inch inboard of WS 34. An overall view of the transverse fracture at 1 inch outboard of the left WS 34 is shown in figure 40 showing the inboard side of the fracture as received. The transverse fracture at this location intersected a slosh hole in the center of the web for the Z-stringer, and as indicated in figure 40, the slosh hole was filled with sealant. Figure 41 shows an overall view of the Z-stringer with mating sides of the fractures shown in close proximity after removal from the skin and cutting to facilitate the fractographic examination.

A view of the mating sides of the transverse fracture through the rear Z-stringer intersecting the slosh hole is shown in figure 42. Flat fracture features in a plane perpendicular to the longitudinal axis of the stringer with curving crack arrest lines, features consistent with fatigue, were observed on most of the fracture surface. Fatigue features emanated from the slosh hole area as indicated with unlabeled arrows in figure 42.

A closer view of the outboard surface of the transverse fracture through the Z-stringer at the slosh hole is shown in figure 43. On the upper side of the slosh hole, fatigue features emanated upward through the web and forward through the upper flange to within approximately 0.03 inch of the forward edge of the flange. At the lower side of the slosh hole, fatigue features emanated downward through the web and aft through approximately half the lower flange. At that point, the fracture turned abruptly and intersected a fastener hole in the lower flange. Fatigue features were also observed emanating from the aft side of this fastener hole, extending aft up to 0.095 inch from the hole surface.

Sealant was removed from the stringer surfaces adjacent to the fracture surface and around the slosh hole. The sealant was cut with a knife, pulled with pliers, and scraped from the surface using wood and plastic instruments. Closer views of the fracture surfaces near the slosh hole after removing the sealant are shown in figures 44 and 45. Fatigue origins were located at the slosh hole bore. Some grinding or sanding marks were observed in the area of the slosh hole, but as is apparent in the web profile in the plane of fracture, the web was not thinned at the edge of the hole to the extent that it was thinned at the upper side of the hole for the rear Z-stringer fracture 1 inch outboard of right WS 34 (figure 30).

Overall views of the mating fracture surfaces of the rear Z-stringer fracture just inboard of left WS 34 are shown in figure 46. Fracture through the upper flange and web occurred directly adjacent to the left WS 34 rib. Fracture through the lower flange occurred approximately 1 inch inboard of left WS 34, and the fracture between the lower flange and

the web was connected by a length of longitudinal fracture in the transition radius between the lower flange and the web. An area of flat fracture with arrest lines consistent with fatigue was observed in the lower flange as indicated in figure 46. The fatigue features emanated forward from a fastener hole in the lower flange for a fuselage attachment angle fastener. The forward boundary of the fatigue region was located at the edge of the transition radius to the stringer web. The remainder of the fracture in this area had an irregular and rough appearance consistent with overstress fracture. However, significant corrosion was observed in the area of the fracture for the Z-stringer where flakes of corroded material would easily pop from the surfaces in and around the fracture.

Middle Z-stringer

The middle Z-stringer had a transverse fracture located 3.75 inches outboard of left WS 48, and an overall view of the inboard side of the fracture is shown in figure 47. Most of the fracture features were on slant angles consistent with overstress, but two areas in the upper flange as indicated in figure 47 had flat fatigue features emanating from a fastener hole.

A closer view of the areas of fatigue is shown in figure 48. A dashed line in figure 48 indicates the forward boundary of the fatigue region at the forward side of the hole. An unlabeled arrow indicates a much smaller fatigue region observed emanating up to 0.015 inch aft from the lower aft side of the hole.

The slosh hole opening for the middle Z-stringer 1 inch outboard of WS 34 was filled with sealant. Sealant was removed from the area of the slosh hole by cutting with a knife, peeling with pliers, and scraping with wood and plastic instruments. The edges of the slosh hole were examined for cracks using an optical stereomicroscope, and no evidence of cracking was observed.

Front Z-stringer

The front Z-stringer had a transverse fracture through the slosh hole, located 1 inch outboard of left WS 34, and another fracture that was located 0 to 3 inches inboard of left WS 34. Fracture features were rough and on slant angles, consistent with overstress fracture. No evidence of fatigue was observed. The entire slosh hole opening was filled with sealant.

Front Spar Lower Spar Cap

The front spar lower spar cap had a transverse fracture approximately 5 inches outboard of left WS 34. A view of the outboard side of the fracture is shown in figure 49. A portion of the fracture surface was relatively flat and perpendicular to the longitudinal axis with crack arrest marks, features consistent with fatigue. Fatigue features emanated from a hole for a threaded fastener to attach a wing leading edge panel. A closer view of the fatigue origin area after removal of the threaded fastener is shown in figure 50. Pitting and

thinning of the flange was observed at the upper surface around the hole, and the thinned area was filled with black sealant as shown in figure 50.

The fatigue features emanated aft, intersecting the forward outboard side of a fastener hole for a skin panel fastener. Multiple fatigue initiation sites were observed at the aft side of the skin panel fastener hole, and fatigue features emanated aft to the boundary indicated by the dashed line in figure 49. The fatigue region on the aft side of the skin fastener hole contained multiple rough, darker gray fracture regions, indicative of faster propagation or overstress fracture, interspersed between lighter colored regions with crack arrest positions.

The front spar lower spar cap was also fractured at a location 1 to 3 inches inboard of left WS 34. Fracture features were rough and on slant angles, consistent with overstress fracture. Corrosion and loss of thickness was observed in the spar cap in the area of the fracture.

Lower Skin

An overall view of the lower skin panel with doublers and stiffeners removed is shown in figure 51. Around the skin repair filler piece, no discernable fracture features were observed. The edges of the skin around the filler were rubbed and/or cut or were covered with primer.

Most of the skin fracture surfaces were relatively rough and on slant angles, consistent with overstress. However, several areas with fatigue features (flat fracture perpendicular to the skin surface with curving crack arrest lines) were observed at the inboard fracture surface as indicated with unlabeled brackets in figure 51. More details of the fracture observations at the inboard fracture surface are provided in table 3. On the airplane, all of the fatigue regions in the skin fracture were covered on the outside by the external doubler, but were not covered on the inside by the internal doublers.

Dimensional Measurements

Rear Spar Lower Spar Cap

Flange thickness of the rear spar lower spar cap was measured in areas that appeared relatively clean and in areas that were corroded and/or had tool marks. Thickness measurements were taken with a point micrometer at the upper end of the vertical flange, at the forward end of the horizontal flange, and in areas of pitting where noted. Results of the measurements are shown in table 4. According to the engineering drawing for the rear spar lower spar cap, the thickness of the vertical flange should be $\frac{1}{2}$ inch and, at its forward edge, the horizontal flange should be $\frac{1}{4}$ inch.

Rear Z-stringer

Flange and web thickness of the rear Z-stringer was measured in areas that appeared relatively clean and in areas that were corroded and/or had tool marks. Thickness measurements were taken with a point micrometer near the center of the web or flange. Results of the measurements are shown in table 5. As measured from a full-scale engineering blueprint of the rear z-stringer, the thicknesses of the flanges and web of the z-stringers are designed to be approximately 0.09 inch thick each.

Table 3. Skin Fracture Features Inboard of Left WS 34

Distance from Aft Edge of Skin (inches)	Fracture Features Consistent With:	Fracture Observations
0 - 1.75	Overstress	Slant angle, intersects fastener hole for rear spar lower spar cap
1.75 – 2.7	Fatigue	Flat fracture emanating aft from fastener hole
2.7 – 2.9	Fastener hole	Threaded external doubler fastener
2.9 – 3.9	Fatigue	Flat fracture emanating forward from fastener hole
3.45 – 3.95	Fatigue	Flat fracture emanating aft from fastener hole
3.95 – 4.15	Fastener hole	Threaded external doubler fastener
4.15 – 5.0	Fatigue	Flat fracture emanating forward from fastener hole
5.0 – 5.15	Overstress	Slant angle
5.15 - 5.4	Fastener hole	Threaded external doubler fastener
5.4 – 5.6	Fatigue	Relatively rough, transitioning to slant angle
5.6 – 6.1	Overstress	Slant angle
6.1 – 6.4	Damage	Post fracture damage
6.4 – 6.7	Fatigue	Flat fracture emanating aft from fastener hole
6.7 – 6.9	Fastener hole	Threaded external doubler fastener
6.9 – 7.55	Fatigue	Flat fracture emanating forward from fastener hole
7.55	Overstress	Abrupt step intersecting outboard side of fastener hole
7.55 – 7.65	Fastener hole	Threaded fastener for external doubler
7.65 – 7.8	Fatigue	Flat fracture emanating forward from fastener hole
7.8 +	Overstress	Slant angle for remaining fracture forward of 7.8 inches

Table 4. Rear Spar Lower Spar Cap Dimensional Measurements

Wing Station	Flange	Thickness (inches)	Comments
Centerline	Horizontal	0.259	Clean
Centerline	Vertical	0.480	Clean
Right WS 34	Horizontal	0.249	Corroded area
Right WS 34	Horizontal	0.230	Corroded area adjacent to fracture surface
Right WS 34	Vertical	0.478	Clean
Right WS 34	Vertical	0.437	In pit near threaded fastener hole
Right WS 40	Horizontal	0.249	Clean
Left WS 29	Horizontal	0.242	Corroded area
Left WS 29	Vertical	0.480	Corroded area
Left WS 32	Horizontal	0.203	Corroded area
Left WS 34	Horizontal	0.211	Corroded area
Left WS 40	Horizontal	0.247	Clean

Table 5. Rear Z-stringer Dimensional Measurements

Wing Station	Flange or Web	Thickness (inches)	Comments
Right WS 29	Upper	0.091	Clean
Right WS 29	Web	0.0875	Clean
Right WS 29	Lower	0.091	Clean
Right WS 34	Upper	0.094	
Right WS 34	Web	0.080	Corrosion
Right WS 34	Lower	0.086	Corrosion
Right WS 35	Upper	0.089	Adjacent to fracture
Right WS 35	Web	0.089	Adjacent to slosch hole
Right WS 35	Lower	0.087	Adjacent to fracture
Left WS 11	Upper	0.093	Clean
Left WS 11	Web	0.089	Clean
Left WS 11	Lower	0.091	Clean
Left WS 35	Upper	0.089	Adjacent to fracture
Left WS 35	Web	0.084	Adjacent to slosch hole
Left WS 35	Lower	0.087	Adjacent to fracture

Front Spar Lower Spar Cap

The thickness of the front spar lower spar cap flanges was measured in an area near the transverse fracture at 5 inches outboard of left WS 34. The horizontal flange thickness was 0.200 inch as measured in line with the aft fastener row consisting of skin panel fasteners. The vertical flange thickness was 0.188 inch. As measured from a full-scale engineering blueprint of the front spar lower spar cap, the thicknesses of the horizontal and vertical flanges of the spar cap is designed to be approximately 0.2 inch and 0.19 inch, respectively.

Lower Skin

The thickness of the skin was measured in multiple locations including relatively clean areas and in areas of corrosion and/or tool marks. According to stress notes for the Grumman G-73 wing, the skin thickness for the Grumman model G-73 airplane is 0.052 inch. At right WS 16, the skin appeared clean and had a thickness of 0.052 inch. At a location just outboard of the crack in the repair area adjacent to WS 34, the skin thickness was 0.045 inch thick. At a location adjacent to the skin fracture within the repair area adjacent to WS 34, the skin thickness was 0.48 inch. Within the localized reduced thickness area of the whirl pattern shown in figure 10 in the repair area adjacent to WS 34, the skin thickness was 0.024 inch.

Near left WS 34, the skin thickness was 0.040 inch adjacent to the inboard fracture. The skin repair filler piece measured 0.047 inch thick. In a corrosion pit in the skin just inboard of the repair filler piece, the skin thickness 0.009 inch.

Repair Doublers

In the repair area adjacent to right WS 34, the inboard edges of the repair doublers were located adjacent to the rib at right WS 34. The external doubler measured 19.5 inches chordwise, 4 inches spanwise, and 0.0625 inch thick. The internal doublers consisted of 3 separate pieces located between stiffeners that covered a total area 17.5 inches chordwise and 3.75 to 4.25 inches spanwise. The rear internal doubler had a jog at its forward end, and the horizontal flange for the rear Z-stringer was partially covered by the internal doubler as shown in the schematic drawing in figure 19. The forward edge of the middle Z-stringer was adjacent to the horizontal flange for the middle Z-stringer and did not cover the flange. The rear, middle, and front internal doublers were 0.046 inch, 0.0605 inch, and 0.066 inch thick, respectively.

In the repair area at left WS 34, the external doubler had a chordwise dimension of 7.25 inches at its aft edge, a spanwise dimension of 12.75 inches outboard of WS 34, and a thickness of 0.085 inch. The external doubler was continuous across WS 34, and its inboard edge was located approximately 3 inches inboard of WS 34. The forward portion of the external doubler had a 1.5 inch wide strip that was sandwiched between the skin panel and the fuselage attachment angle.

Two internal doublers were also present in the repair area at left WS 34. The rear internal doubler located between the rear spar lower spar cap and the rear Z-stringer measured 5.5 inches chordwise, 6 inches spanwise, and 0.048 inch thick. The front internal doubler located forward of the rear Z-stringer measured 4 inches chordwise, 3.75 inches spanwise, and 0.042 inches thick. As shown in the schematic drawing in figure 38, the rear doubler spanned across left WS 34, and its inboard edge was located approximately 2 inches inboard of left WS 34. The inboard edge of the front doubler was located adjacent to left WS 34.

Hardness and Conductivity

Hardness and conductivity of samples from the rear spar lower spar cap, rear Z-stringer, and lower skin were measured in selected areas of the carrythrough portion of the wing box beam. The samples of the rear spar lower spar cap, rear Z-stringer, and lower skin were taken from left WS 5, left WS 10, and left WS 3, respectively. Surfaces to be tested were hand ground with up to 600 grit paper to remove surface coatings, oxidation, and in the case of the skin, a layer of cladding. Results of the hardness and conductivity measurements are shown in table 6. The material specifications using designations from the engineering drawings for the three selected structural components are also shown in table 6. For reference, the current Aluminum Association designations that replaced the old designations in the drawing are provided. For further reference, typical values of hardness and conductivity for the specified materials as listed in the *Aerospace Structural Metals Handbook*³ are also provided in table 6.

Table 6. Hardness and Conductivity Measurements

Structural Component	Drawing Spec.	Current Designation	Hardness (HRB)		Conductivity (% IACS)	
			Measured	Typical	Measured	Typical
Spar cap	75 ST	7075-T6	95.1	89*	32.0	30 [†]
Z-stringer	75 ST	7075-T6	95.1	89*	31.7	30 [†]
Skin	R301-T6	2014-T6	81.4	80 – 86	37.5	40 [‡]

* Converted to HRB from reference value of 150 HB.

[†] Converted to % IACS from reference resistivity value of 2.26 microhm-inch.

[‡] Converted to % IACS from reference resistivity value of 1.69 microhm-inch.

Composition

The composition of the rear spar lower spar cap, rear Z-stringer, and lower skin were determined using optical emission spectroscopy. Testing was completed in the areas prepared for hardness and conductivity measurements as described in the previous section of this report. Results showing the composition of the selected components are shown in tables 7 and 8. For reference, the compositions of the 7075 and 2014 aluminum alloys as published in *Aerospace Structural Metals Handbook* are also listed in tables 7 and 8. Composition values shown in bold in table 7 were outside the reference composition limits.

³ *Aerospace Structural Metals Handbook*, Edited by W. F. Brown, Jr., H. Mindlin, and C. Y. Ho, CINDAS/Purdue University (1995).

Table 7. Composition of the Lower Spar Cap and Z-stringer

Element	Measured Composition (weight percent)		Reference 7075 Composition (weight percent)
	Spar Cap	Z-stringer	
Copper	1.60	1.56	1.2 – 2.0
Magnesium	2.63	2.69	2.1 – 2.9
Manganese	0.17	0.14	<0.3
Iron	0.41	0.33	<0.7
Silicon	0.18	0.12	<0.5
Zinc	7.14	7.13	5.1 – 6.1
Chromium	0.31	0.29	0.18 – 0.4
Titanium	0.04	0.03	<0.2
Others each*	<0.04	<0.06[†]	<0.05
Others total*	0.10	0.11	<0.15

*"Others each" is the individual composition of each of elements not specifically listed, and "others total" is the sum total of the composition of those other elements. Other elements tested were calcium, lead, nickel, tin, cobalt, bismuth, cadmium, boron, beryllium, strontium, vanadium, gallium, silver, and zirconium.

[†]Gallium was the only element tested with an individual composition value greater than the reference maximum.

Table 8. Composition of the Lower Skin

Element	Measured Skin Composition (weight percent)	Reference 2014 Composition (weight percent)
Copper	4.42	3.9 – 5.0
Silicon	1.11	0.5 – 1.2
Iron	0.36	<0.7
Manganese	0.94	0.4 – 1.2
Magnesium	0.51	0.2 – 0.8
Zinc	0.095	<0.25
Chromium	0.063	<0.10
Titanium	0.011	<0.15
Others each*	<0.02	<0.05
Others total*	0.07	<0.15

*"Others each" is the individual composition of each of elements not specifically listed, and "others total" is the sum total of the composition of those other elements. Other elements tested were calcium, lead, nickel, tin, cobalt, bismuth, cadmium, boron, beryllium, strontium, vanadium, gallium, silver, and zirconium.

Metallography

Polished cross-sections of the rear spar lower spar cap, rear Z-stringer, and lower skin were prepared for microstructural examination. The cross-section of the rear spar lower spar cap was prepared from a sample selected from left WS 23. This area had

corrosion on the lower surface of the spar cap where it had mated to the skin panel and appeared to be free of grinding or sanding marks. The Z-stringer cross-section was prepared from the upper flange at left WS 10, where hardness, conductivity, and composition measurements were conducted in the web. The cross-section of the lower skin was prepared from a piece cut from right WS 40.

The rear spar lower spar cap was first sectioned with two angled cuts to remove a triangular-shaped piece of the horizontal flange. Another lengthwise cut was made through the horizontal flange, and this surface was polished and etched to reveal the microstructure through the thickness as shown in figures 52 and 53. Typical microstructural features included second phase regions that appeared light gray, dark gray, or orange in the unetched condition and elongated grains that were revealed in the etched condition. A cross-sectional view of the corrosion at the lower surface of the rear spar lower spar cap is shown in figure 54. No cracks were observed in the examined cross-section.

A segment of the upper flange of the rear Z-stringer at left WS 10 was cut lengthwise, and this surface was polished and etched to reveal the microstructure through the thickness of the flange as shown in figures 55 and 56. Typical microstructural features included second phase regions that appeared light gray, dark gray, or orange in the unetched condition and elongated grains that were revealed in the etched condition.

A piece of the lower skin was cut spanwise, and this surface was polished and etched to reveal the microstructures shown in figures 57 and 58. Typical microstructural features included second phase regions that appeared light gray, dark gray, or orange. A clad layer was observed on the skin surfaces as shown in the view in figure 59.

Matthew R. Fox
Senior Materials Engineer

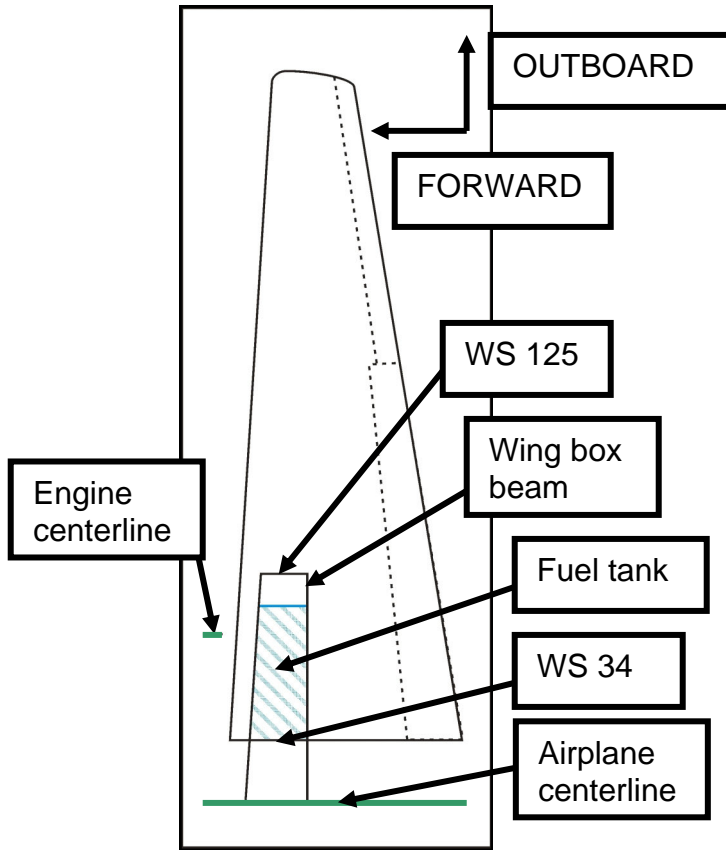


Figure 1. Schematic view of the right wing of the Grumman model G-73 airplane showing the location of the wing box beam.

Image No.:0603A00208, Project No.: 2005120013

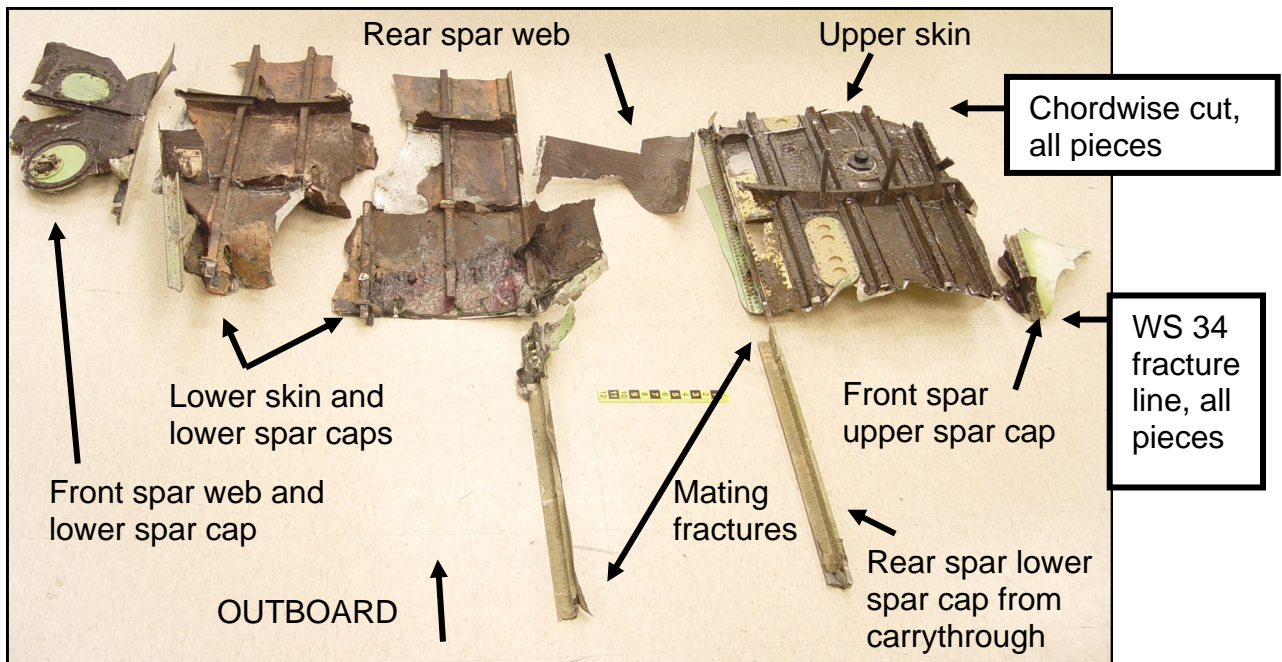


Image No.:0512A00936, Project No.: 2005120013

Figure 2. View of wing box beam pieces from the fractured inboard end of the right wing portion of the wing box beam as received. View is of the internal surfaces opened and laid flat. Pieces of the rear lower spar cap from the carrythrough are also shown.

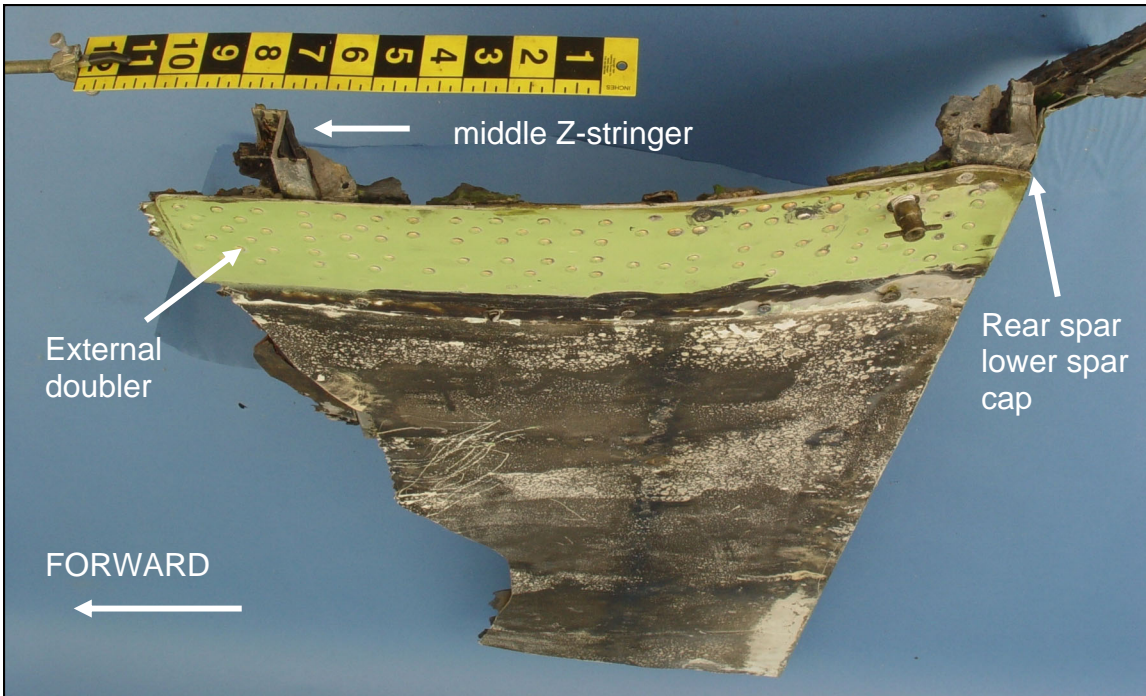


Image No.:0512A00939, Project No.: 2005120013

Figure 3. Aft piece of the lower skin panel and rear spar lower spar cap piece from the right wing pieces shown in the previous figure. View is looking outboard and slightly upward at the lower surface and at fractures at the inboard end near right WS 34.

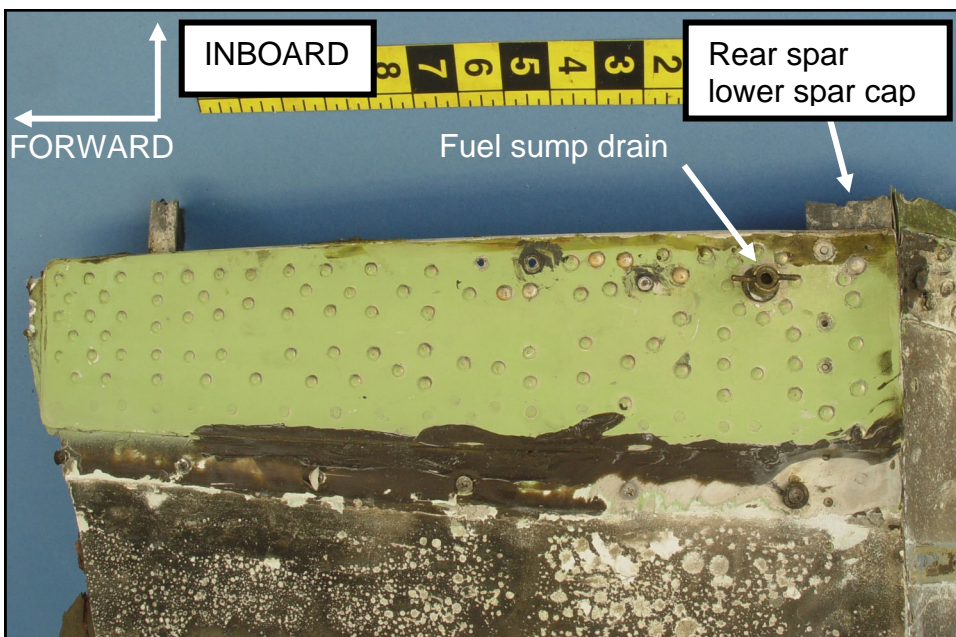


Image No.:0512A00938, Project No.: 2005120013

Figure 4. View of the repair at the inboard end of the wing box beam piece shown in the previous figure. The area with green paint is an external doubler on the lower surface of the skin panel adjacent to right WS 34.

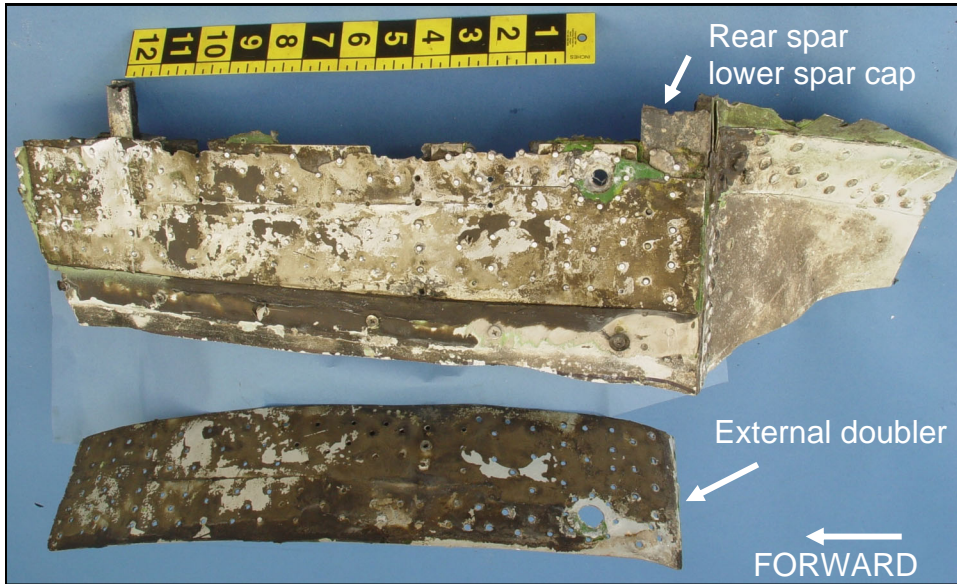


Image No.:0512A00971, Project No.: 2005120013

Figure 5. View of faying surfaces of the lower skin and external doubler shown in the previous figure after removing the external doubler.

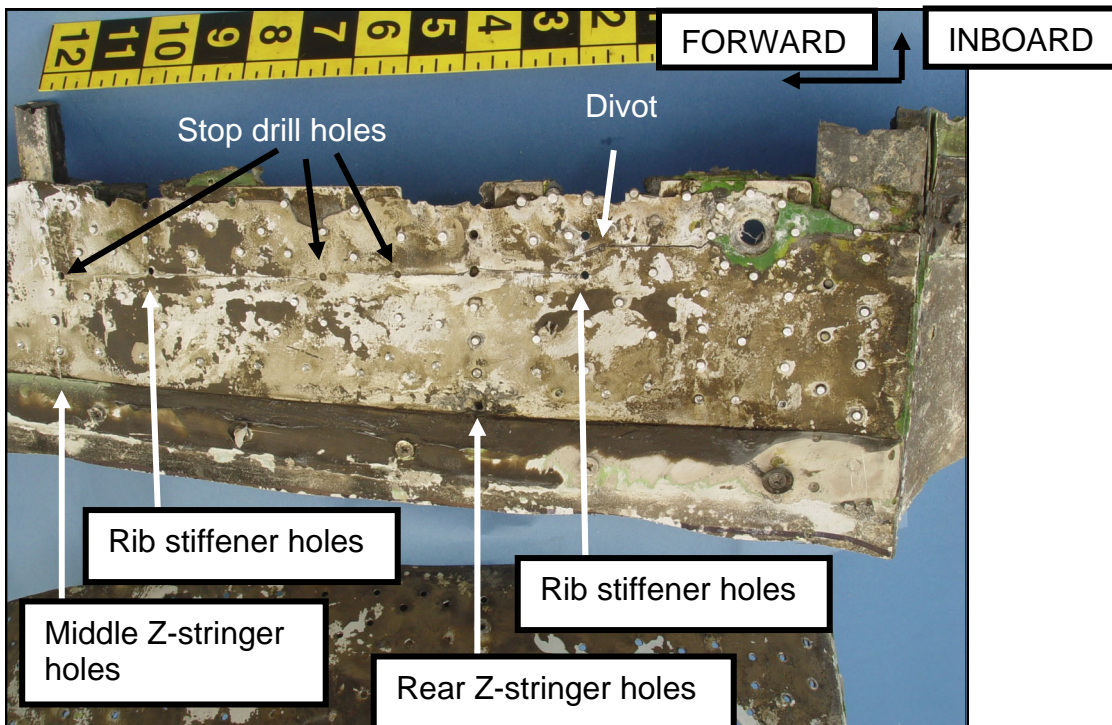


Image No.:0512A00972, Project No.: 2005120013

Figure 6. Closer view of the crack in the lower skin on the piece shown in the previous figure. Holes that the crack intersected forward of the fuel sump drain plate are labeled. The divot was a machined spherical segment of missing material that did not penetrate through the skin thickness.

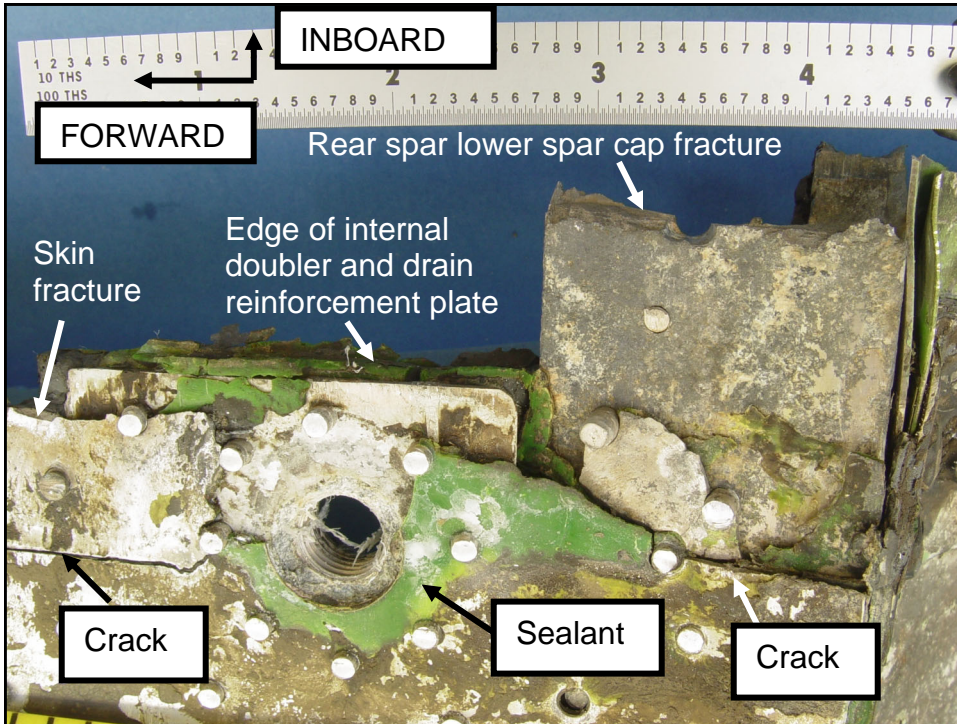


Image No.:0512A00979, Project No.: 2005120013

Figure 7. Closer view of the lower surfaces of the skin and rear spar lower spar cap shown in the previous figure.

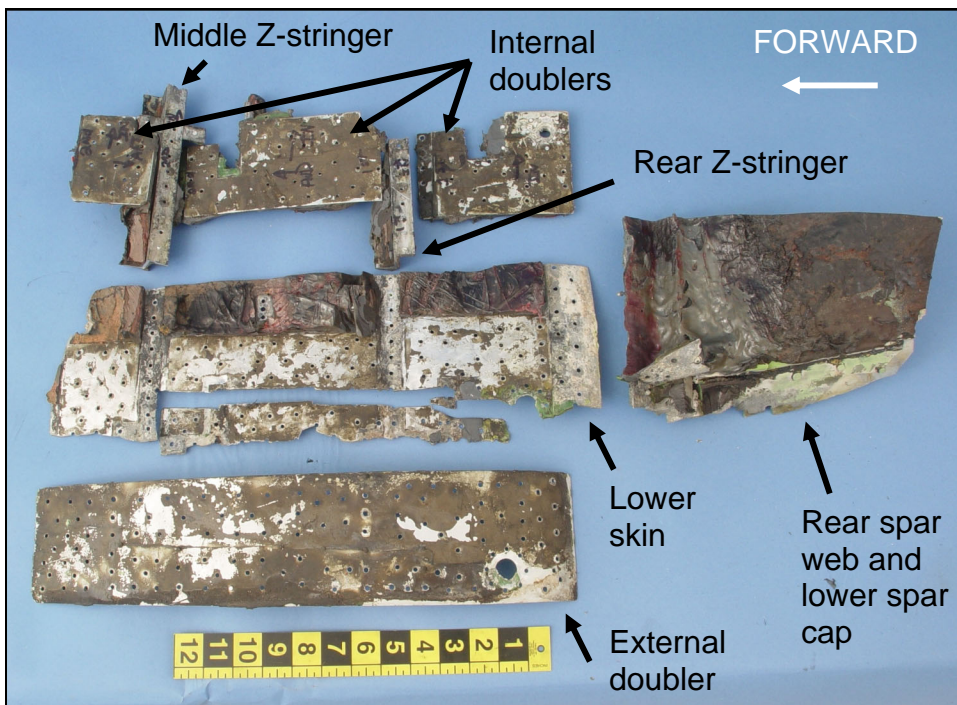


Image No.:0601A00062, Project No.: 2005120013

Figure 8. View of faying surfaces between the right wing lower skin, doublers, and stiffeners in the area of the repair adjacent to right WS 34. For the lower skin, the upper surface is shown.

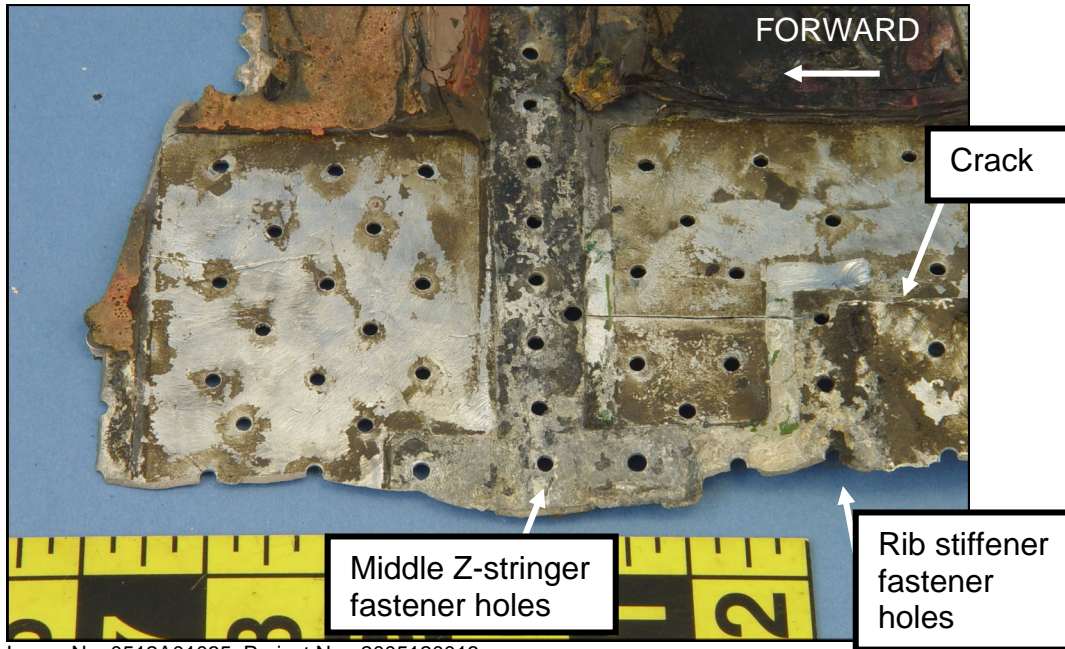


Figure 9. Close view of the upper surface of the lower skin at the middle Z-stringer after removing internal doublers and stiffeners adjacent to right WS 34

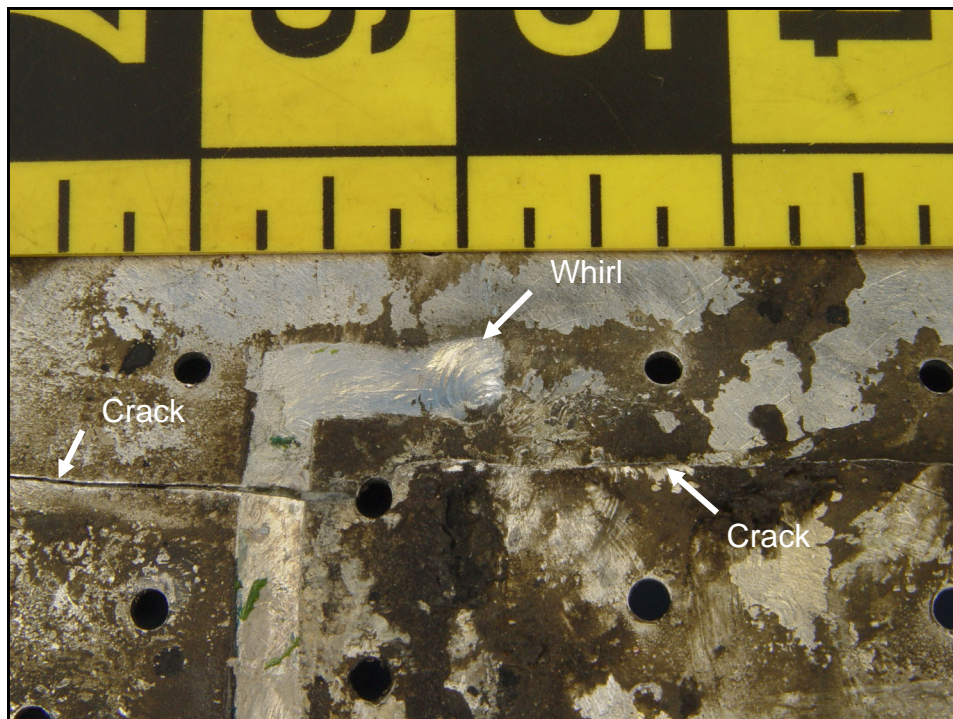


Figure 10. Closer view of the area with a whirl pattern and thinning through the thickness at the edge of the rib stiffener shown in figure 10.

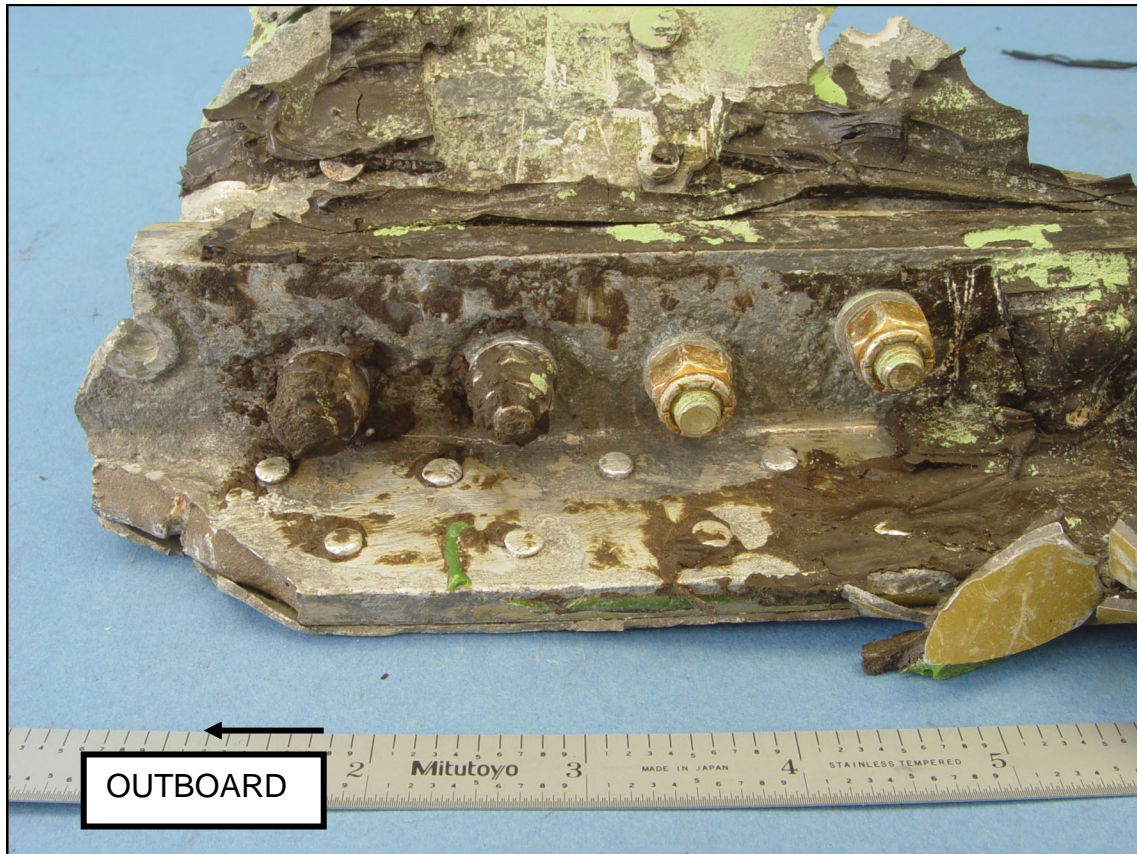


Image No.:0603A00465, Project No.: 2005120013

Figure 11. View of the rear spar lower spar cap adjacent to the fracture location just inboard of right WS 34 after removal of sealant in the area.

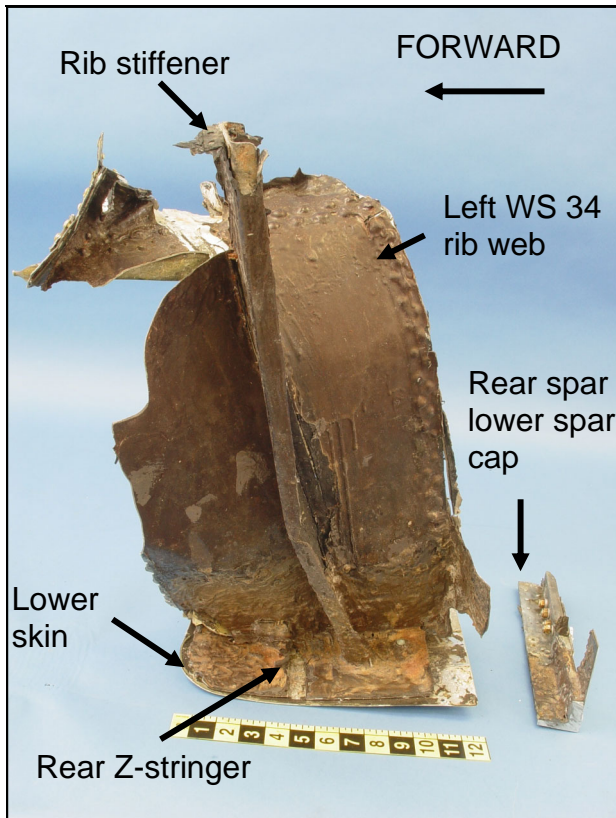


Figure 12. View of the outboard side of wing box beam pieces from the repair area at left WS 34.

Image No.:0601A00086, Project No.: 2005120013

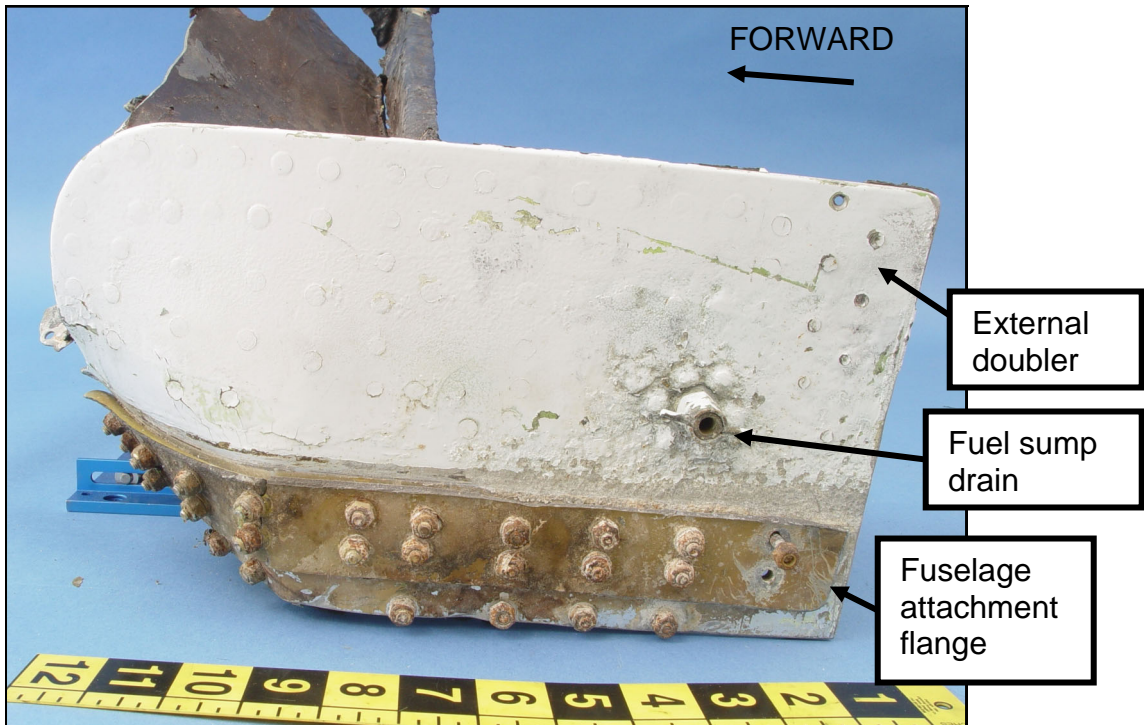


Image No.:0601A00083, Project No.: 2005120013

Figure 13. View of the external doubler and fuselage attachment angle on the lower surface of the left wing piece shown in the previous figure.

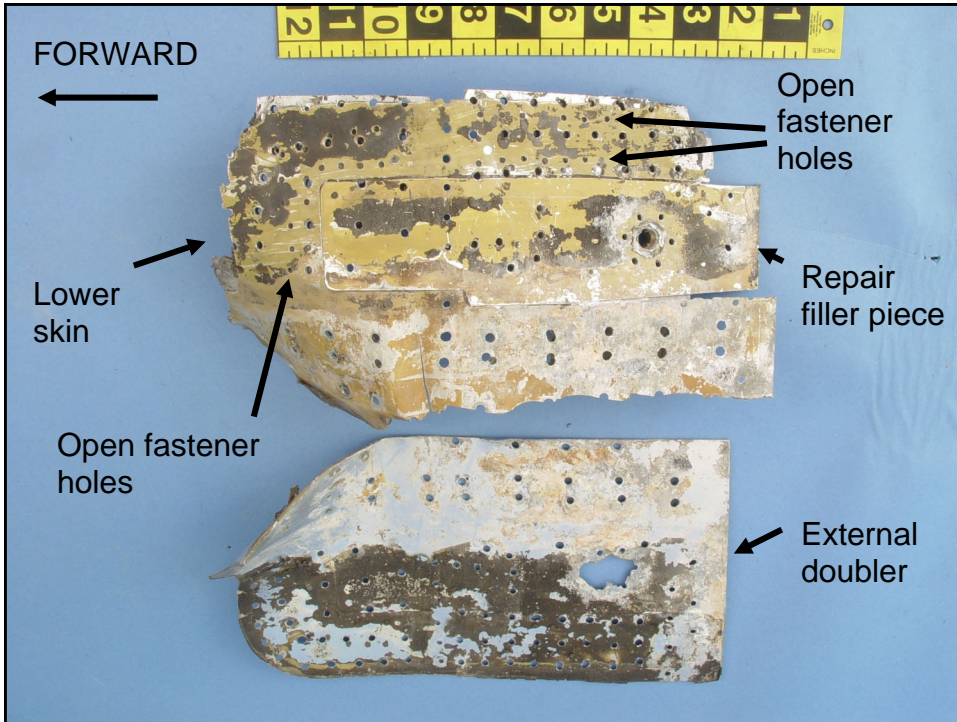


Image No.:0601A00111, Project No.: 2005120013

Figure 14. View of faying surfaces of the lower skin and external doubler after removing the doubler in the repair area at left WS 34.

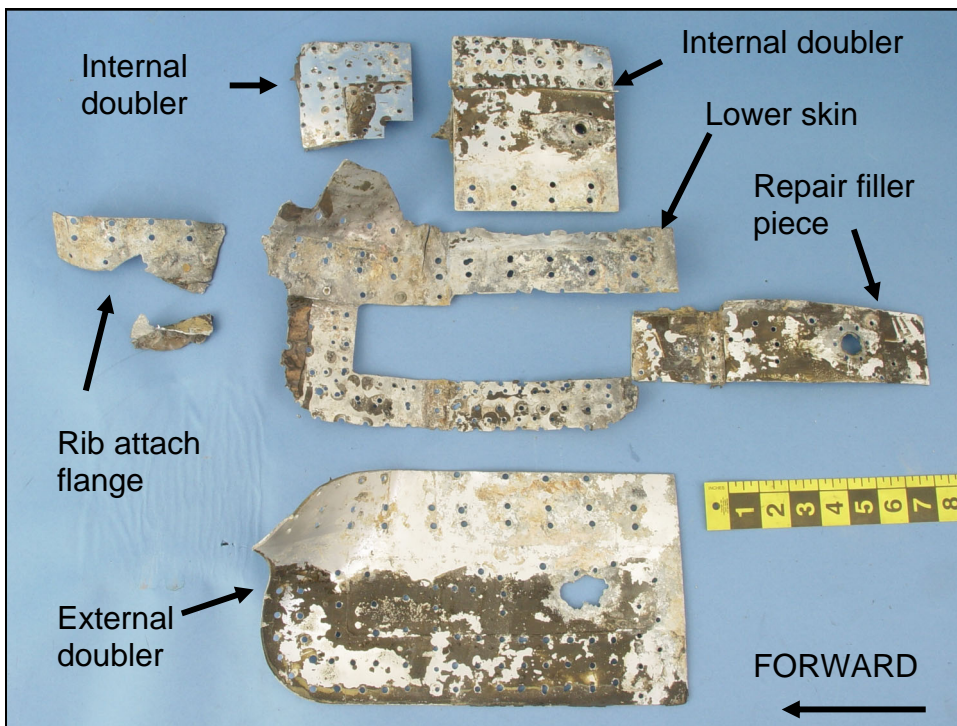


Image No.:0601A00119, Project No.: 2005120013

Figure 15. View of faying surfaces of the left wing lower skin and internal and external doublers at left WS 34. For the lower skin, the upper surface is shown.

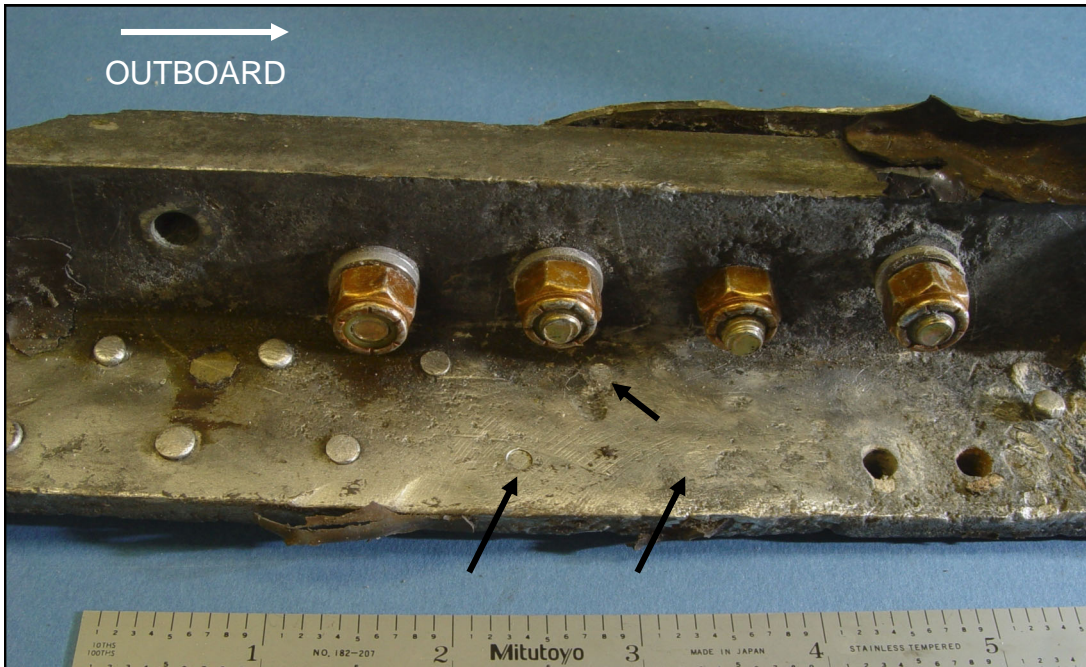


Image No.:0601A01156, Project No.: 2005120013

Figure 16. View of the lower spar cap just inboard of left WS 34 showing grinding or sanding marks and corrosion. Unlabeled arrows indicate rivets with missing tails on the horizontal flange.

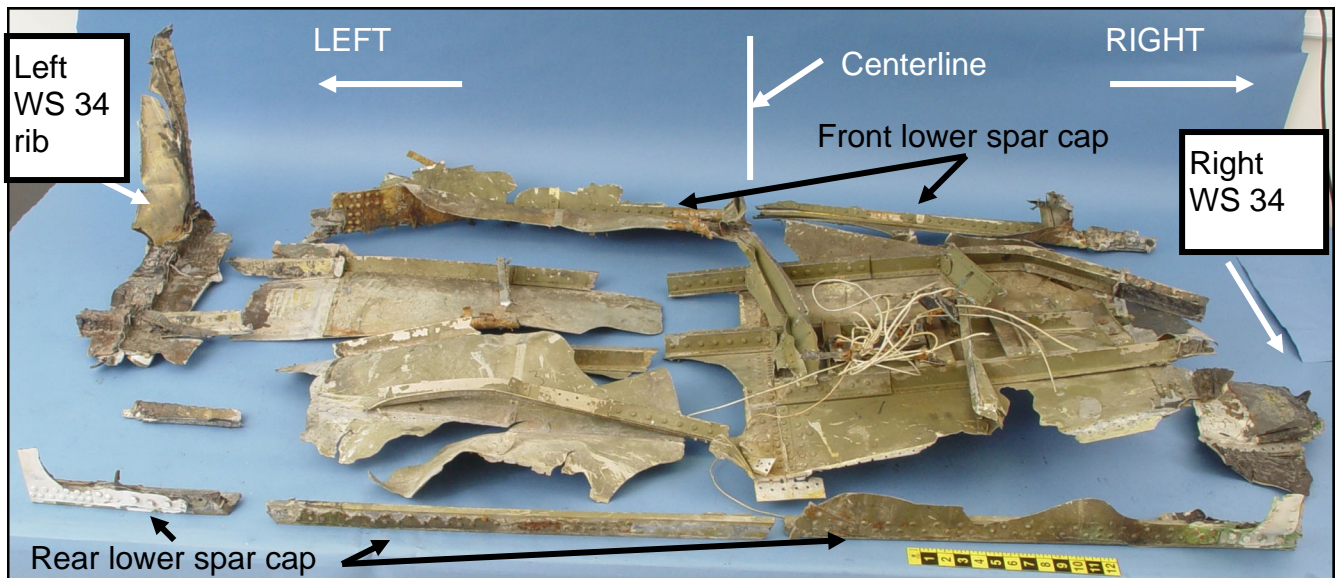


Image No.:0601A00826, Project No.: 2005120013

Figure 17. View of recovered pieces of the lower skin panel and lower spar caps for the carrythrough portion of the wing box beam. View is of the internal surface of the wing box beam pieces viewed looking forward.

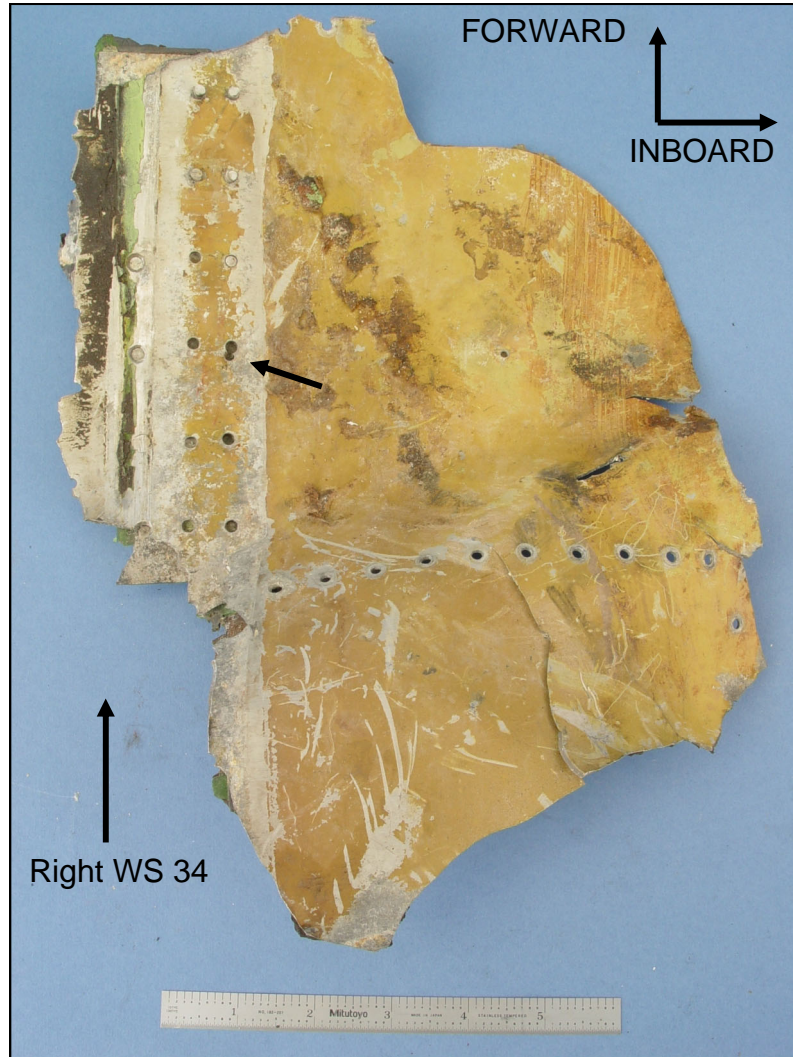


Image No.:0601A01164, Project No.: 2005120013

Figure 18. View of the lower surface of the lower skin at the carrythrough portion of the wing box beam near right WS 34. The unlabeled arrow indicates a double-drilled hole in the inboard fastener hole row for the fuselage attachment angle.

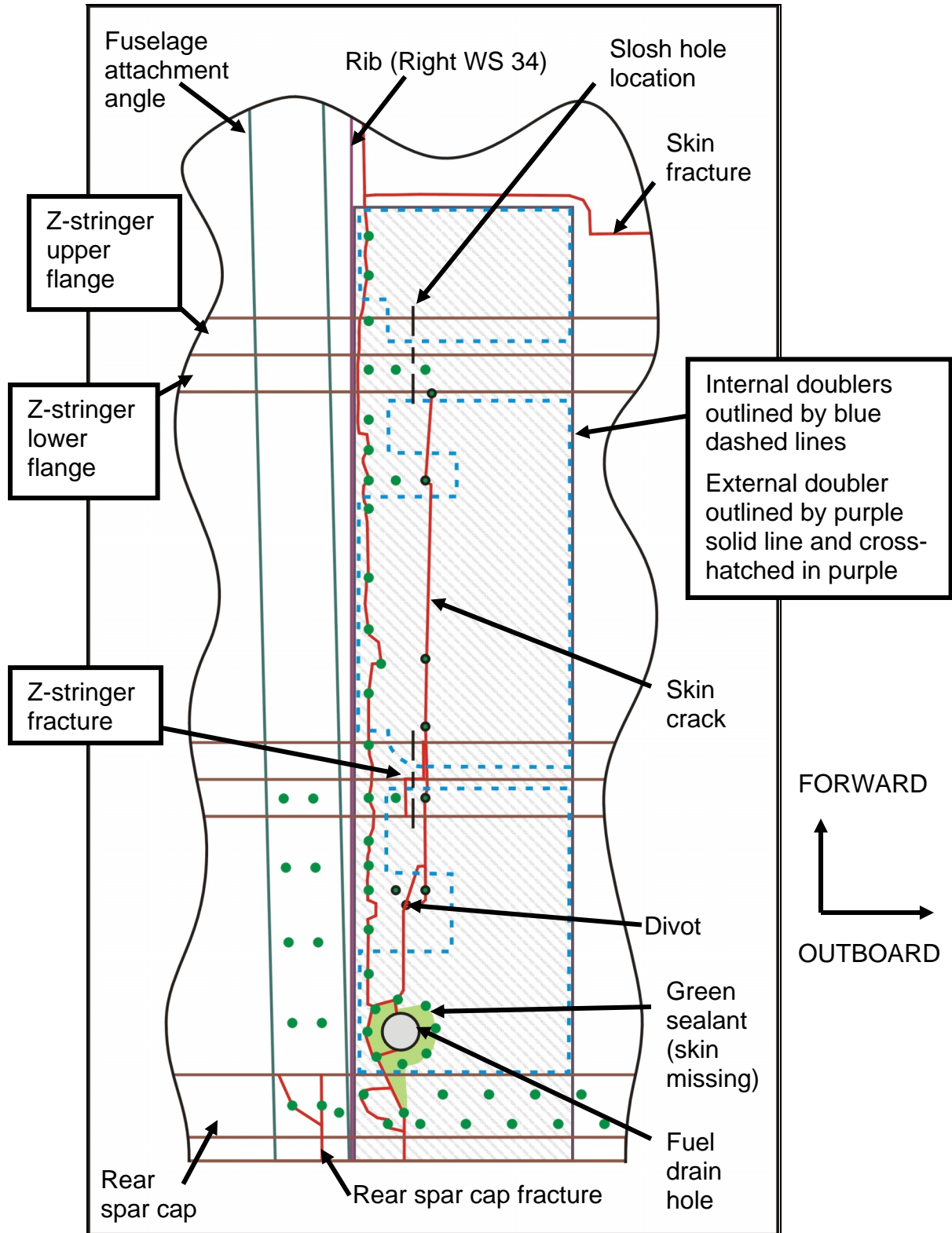


Figure 19. Schematic view of the wing box beam structure including repair doublers at right WS 34. Selected fastener locations are indicated with solid green circles. Circles with black outlines and green centers indicate holes in the skin and/or stringers that did not have fasteners.

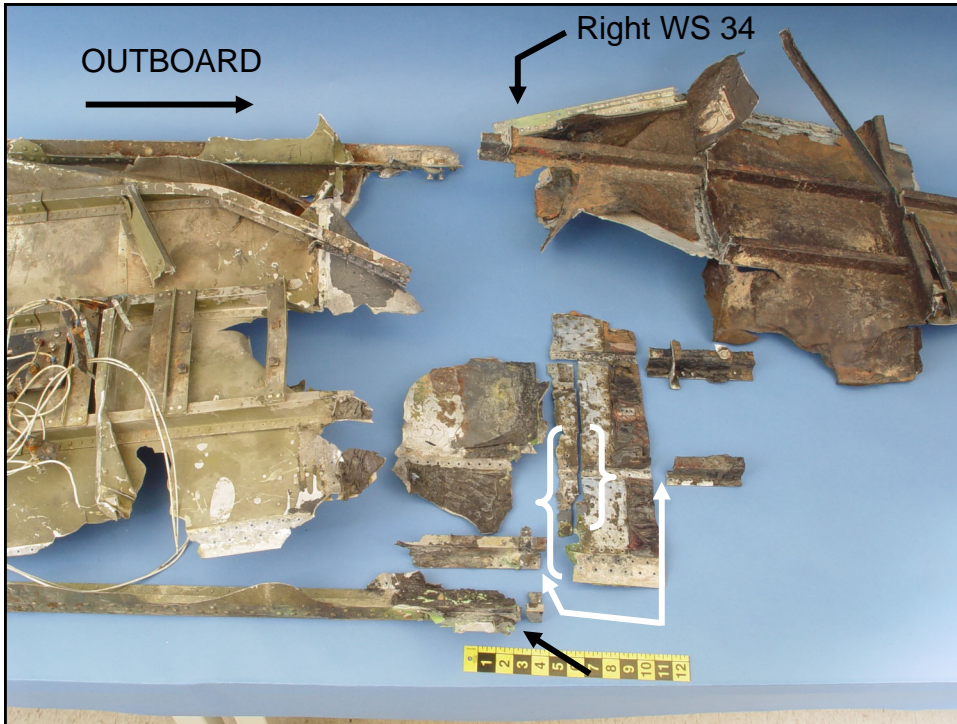


Image No.:0601A00945, Project No.: 2005120013

Figure 20. View of the lower skin and lower spar cap pieces of the wing box beam at right WS 34. Unlabeled arrows and brackets indicate fatigue locations in the skin, rear Z-stringer, and rear spar lower spar cap.



Image No.:0512A00890, Project No.: 2005120013

Figure 21. Close view of the outboard side of the rear spar lower spar cap transverse fracture just inboard of right WS 34. Fatigue features emanated from a double-drilled fastener hole.



Image No.:0512A00893, Project No.: 2005120013

Figure 22. Another view of the rear spar lower spar cap fracture shown in the previous figure. Unlabeled arrows indicate a double-drilled hole.

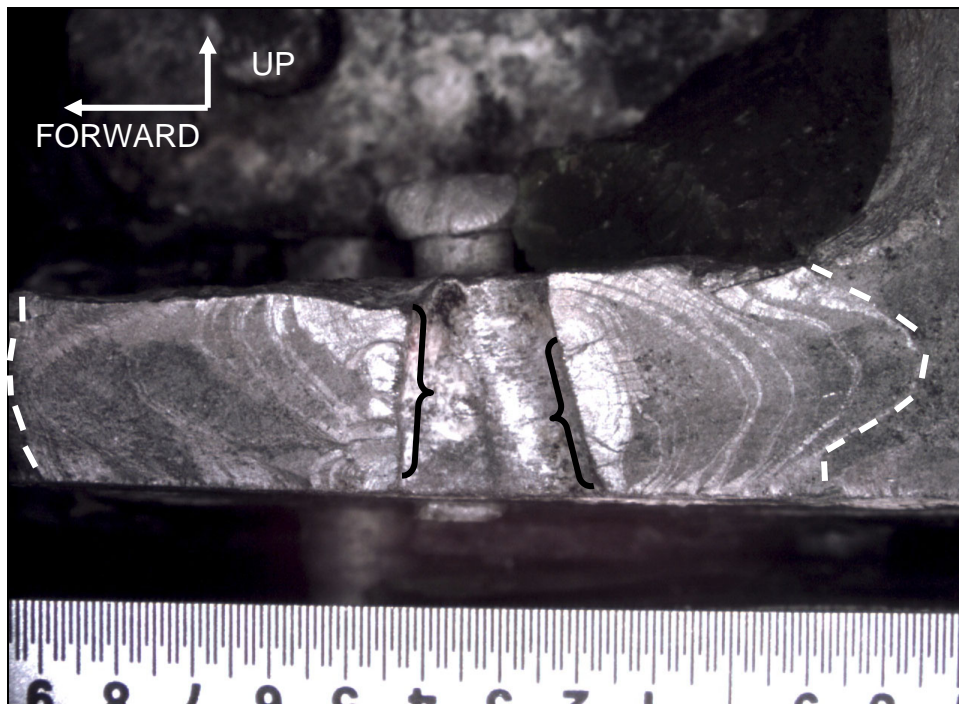


Image No.:0512A00894, Project No.: 2005120013

Figure 23. Closer view of the fatigue region on horizontal flange of rear spar lower spar cap. Dashed lines indicate the fatigue boundaries, and brackets indicate the fatigue origin areas.

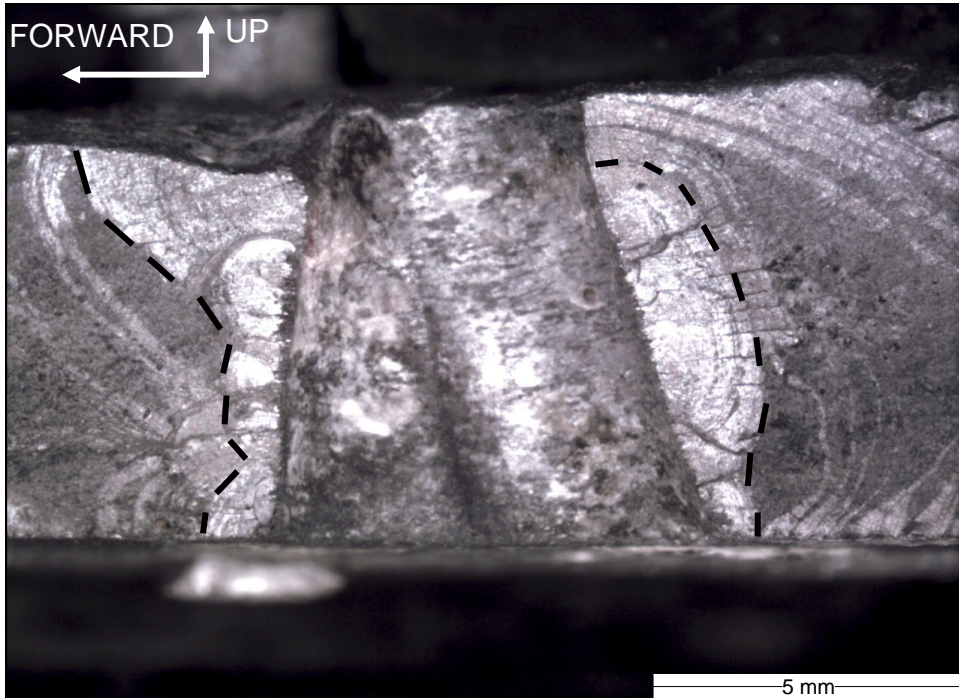


Image No.:0512A00966, Project No.: 2005120013

Figure 24. Closer view of the fatigue origin areas. Dashed lines indicate the extent of flat regions near the origin areas.

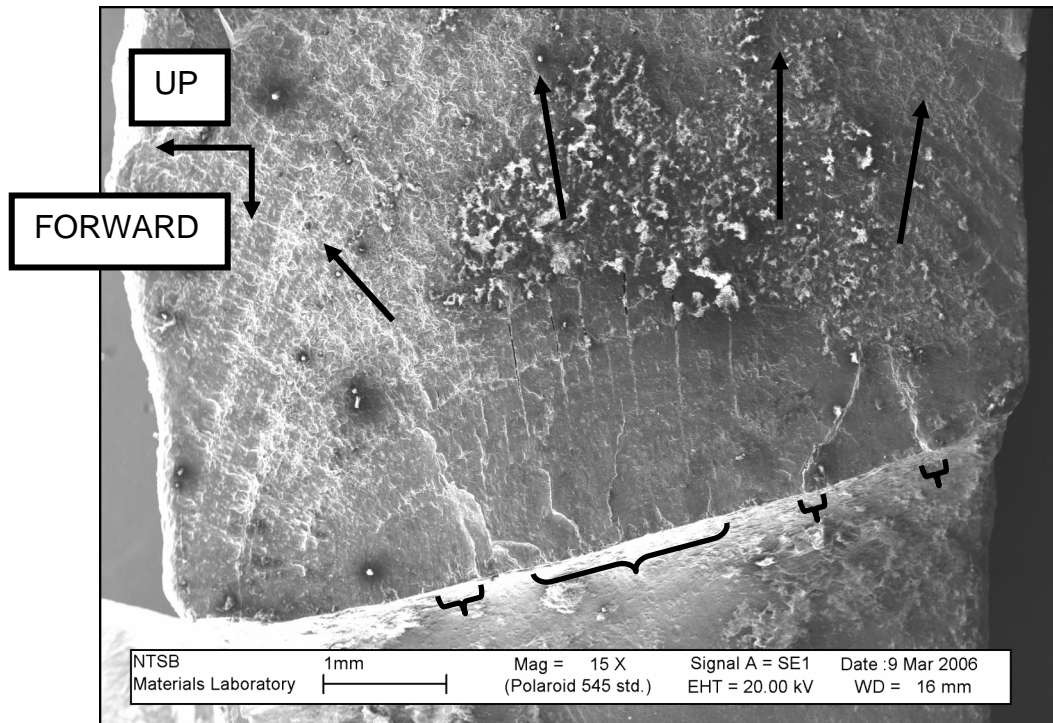


Image No.:0603A00267, Project No.: 2005120013

Figure 25. SEM view of the origin areas at the aft side of the hole. Unlabeled brackets indicate origin areas and unlabeled arrows indicate fatigue propagation directions.

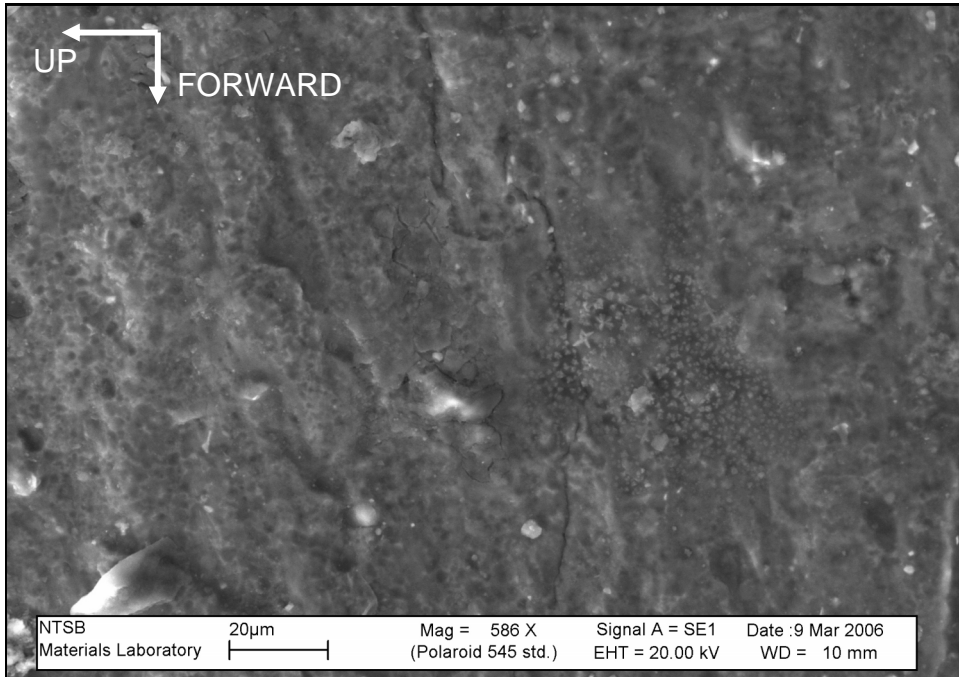


Image No.:0603A00269, Project No.: 2005120013

Figure 26. Closer SEM view of the fracture surface near an origin area at the aft side of the hole showing corrosion and rub damage. Orientation of the spar cap is the same as in the previous figure.

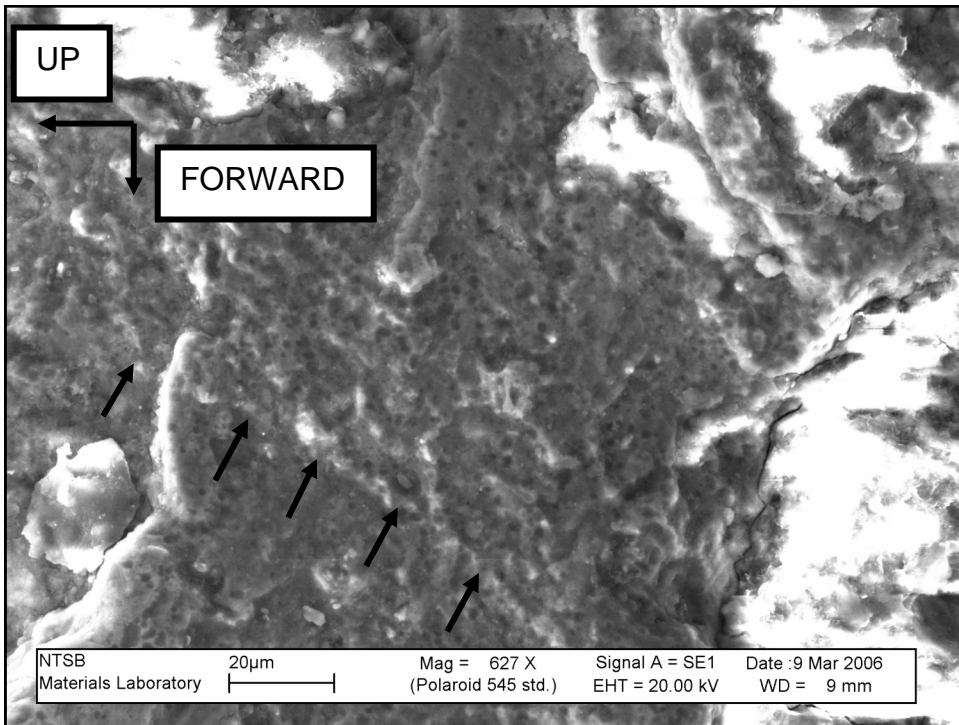


Image No.:0603A00270, Project No.: 2005120013

Figure 27. Close view of fracture features near the fatigue boundary showing corrosion damage. Unlabeled arrows indicate a possible striation.

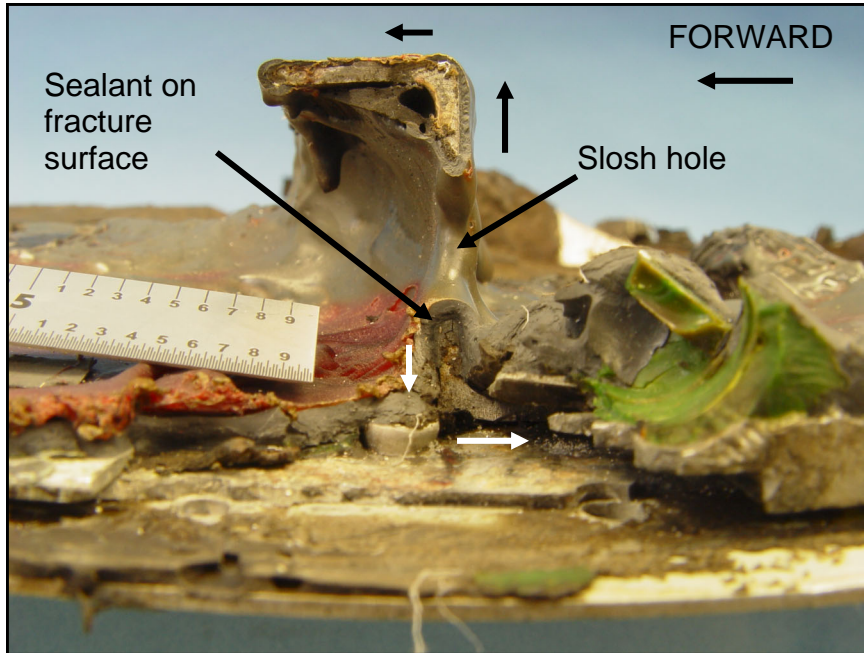


Image No.:0512A00944, Project No.: 2005120013

Figure 28. Close view of the rear Z-stringer fracture near right WS 34. Fatigue features emanated from a slosh hole in the stringer web as indicated with unlabeled arrows.

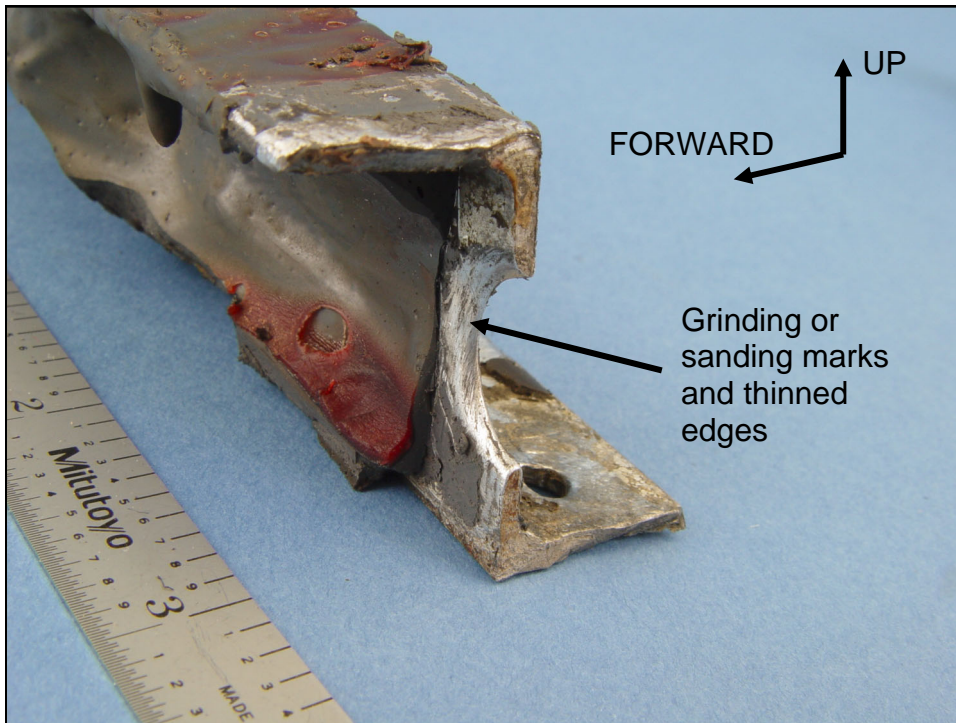


Image No.:0601A01174, Project No.: 2005120013

Figure 29. View of rear Z-stringer fracture near right WS 34 after sealant removal.

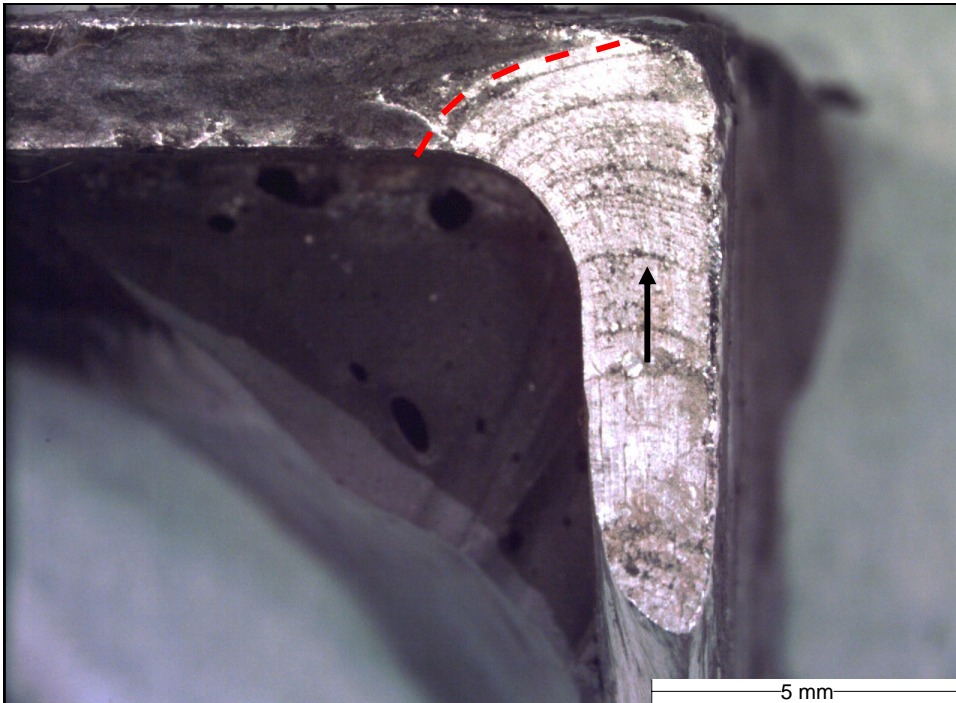


Image No.:0601A01199, Project No.: 2005120013

Figure 30. Close view of fatigue at upper side of hole in rear Z-stringer fracture near right WS 34. A dashed line indicates the fatigue boundary, and an unlabeled arrow indicates the local fatigue propagation direction.

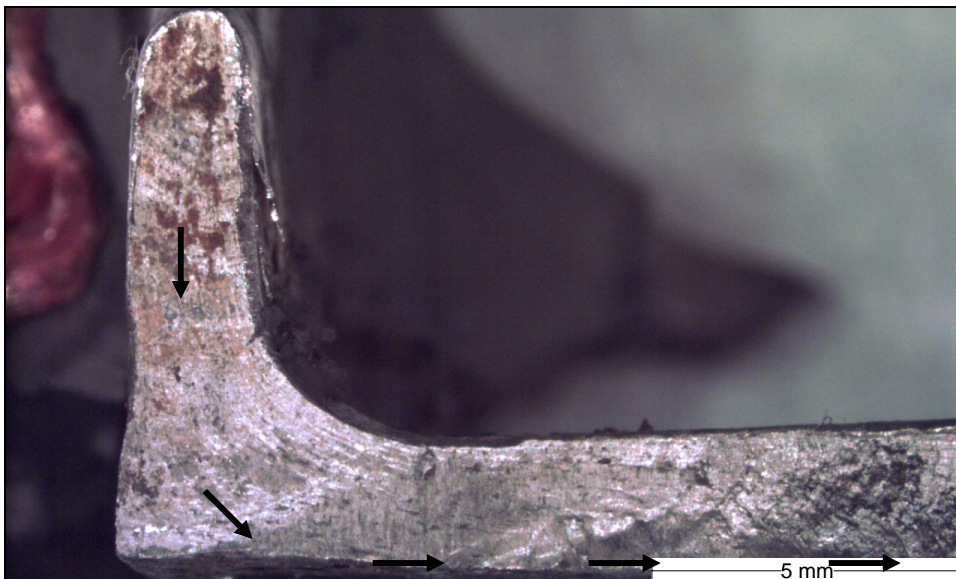


Image No.:0601A01200, Project No.: 2005120013

Figure 31. Close view of fatigue at the lower side of the slosh hole in the rear Z-stringer fracture near right WS 34. Unlabeled arrows indicate the local fatigue propagation directions.

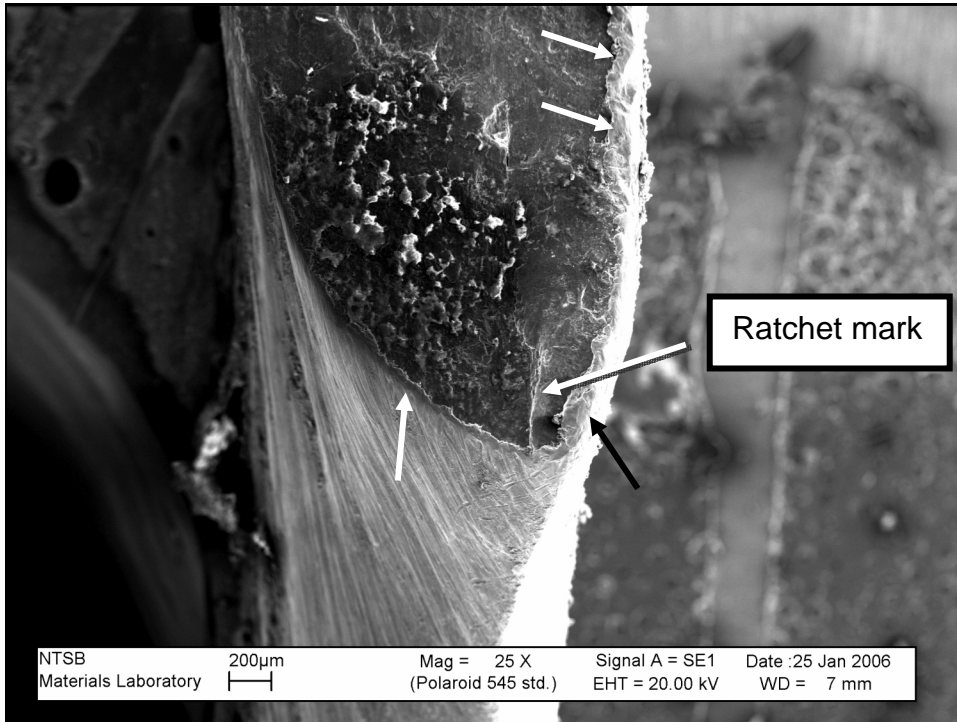


Image No.:0603A00262, Project No.: 2005120013

Figure 32. SEM view of the fatigue origin area at the upper side of the sash hole in the rear Z-string near right WS 34. Unlabeled arrows indicate deformation lips at the edge of the fracture surface.

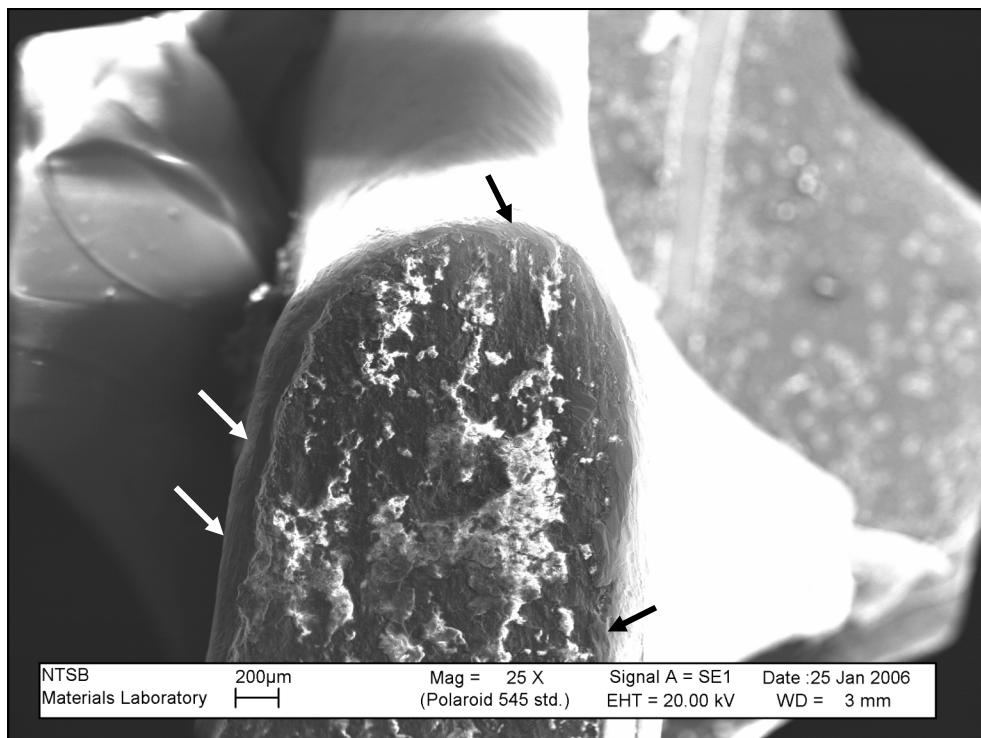


Image No.:0603A00265, Project No.: 2005120013

Figure 33. View of the fatigue origin area at the lower side of the sash hole for the rear Z-stringer fracture near right WS 34. Arrows indicate deformation lips at the edge of the fracture surface.

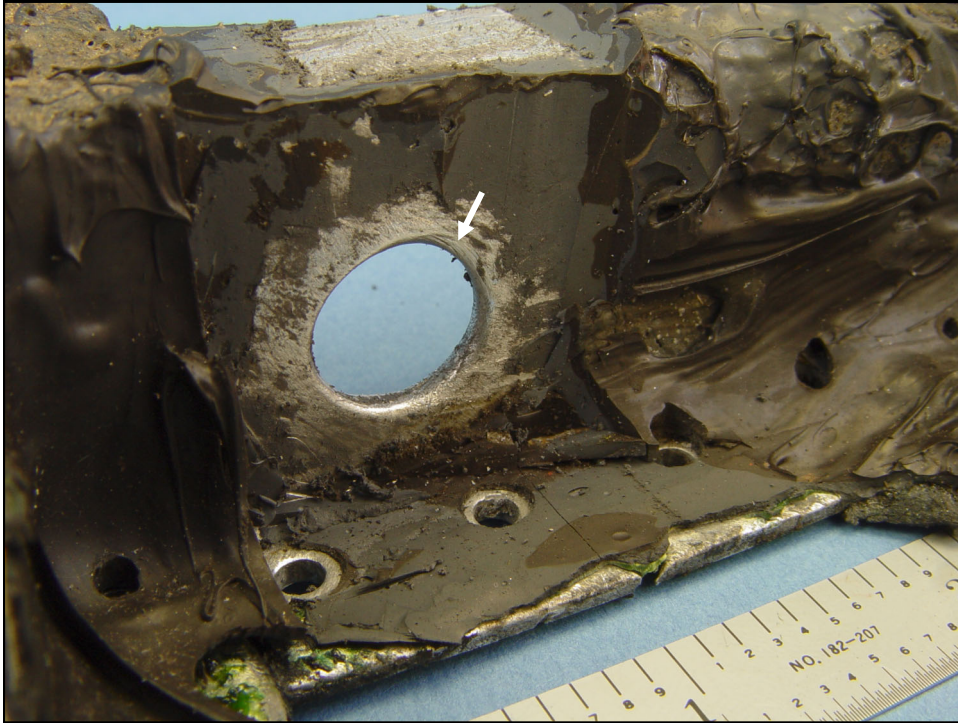


Image No.:0601A01178, Project No.: 2005120013

Figure 34. View of the slosh hole for middle Z-stringer just outboard of right WS 34. An arrow indicates a small area of grinding or sanding marks and thinning at the edge of the hole.

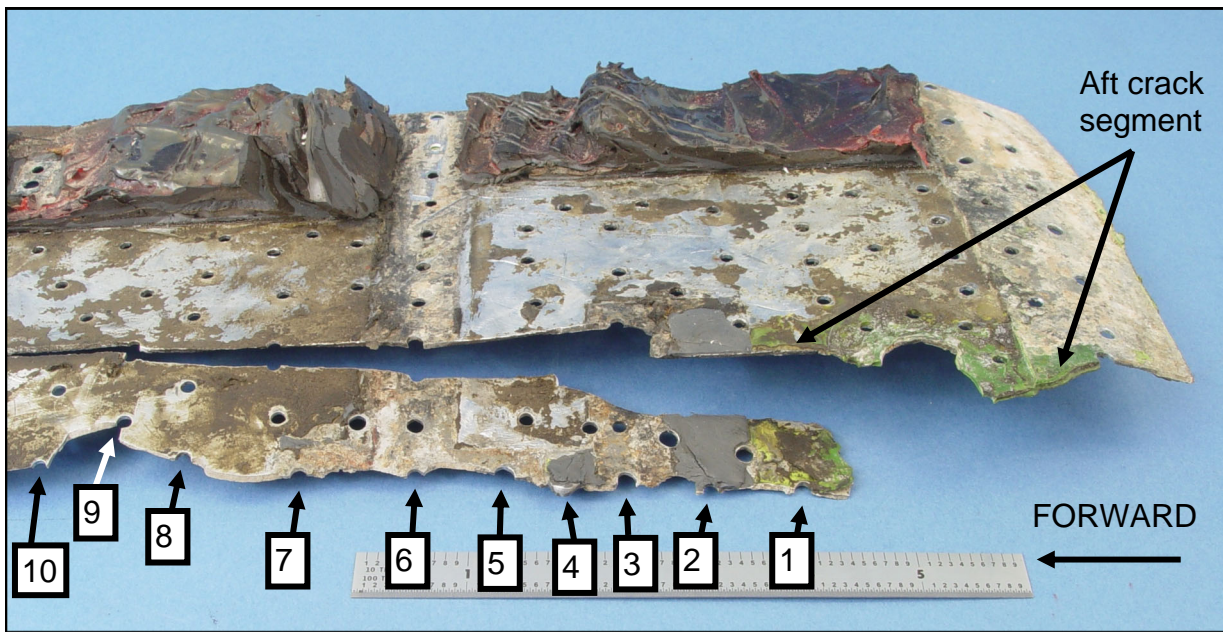


Image No.:0601A01264, Project No.: 2005120013

Figure 35. View of right wing lower skin fracture at inboard fastener holes for doublers. Fastener holes intersected by the skin fracture forward of the green sealant are numbered for reference. Fatigue features were observed emanating from holes 1, 2, 5, 6, 7, and 9.

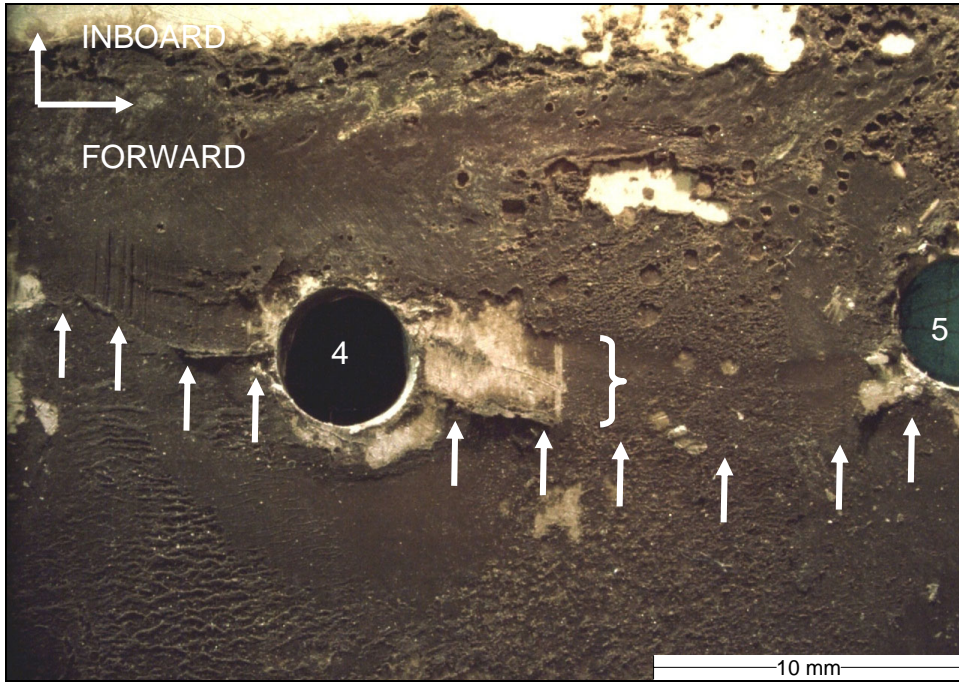


Image No.:0603A00751, Project No.: 2005120013

Figure 36. View of the faying surface of the external doubler near fastener holes 4 and 5. Arrows indicate locations of sealant pushed up at the skin fracture, and a bracket indicates a region of spanwise sliding contact.

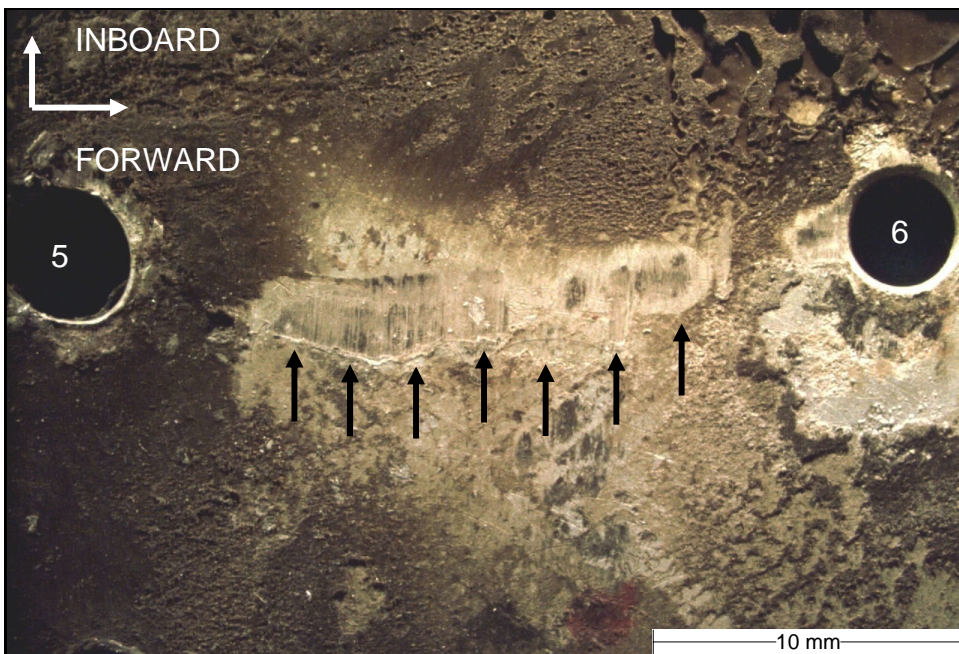


Image No.:0603A00750, Project No.: 2005120013

Figure 37. View of the faying surface of the external doubler between fastener holes 5 and 6. Unlabeled arrows indicate a step in the doubler surface at the skin fracture and spanwise sliding contact marks just inboard of the step.

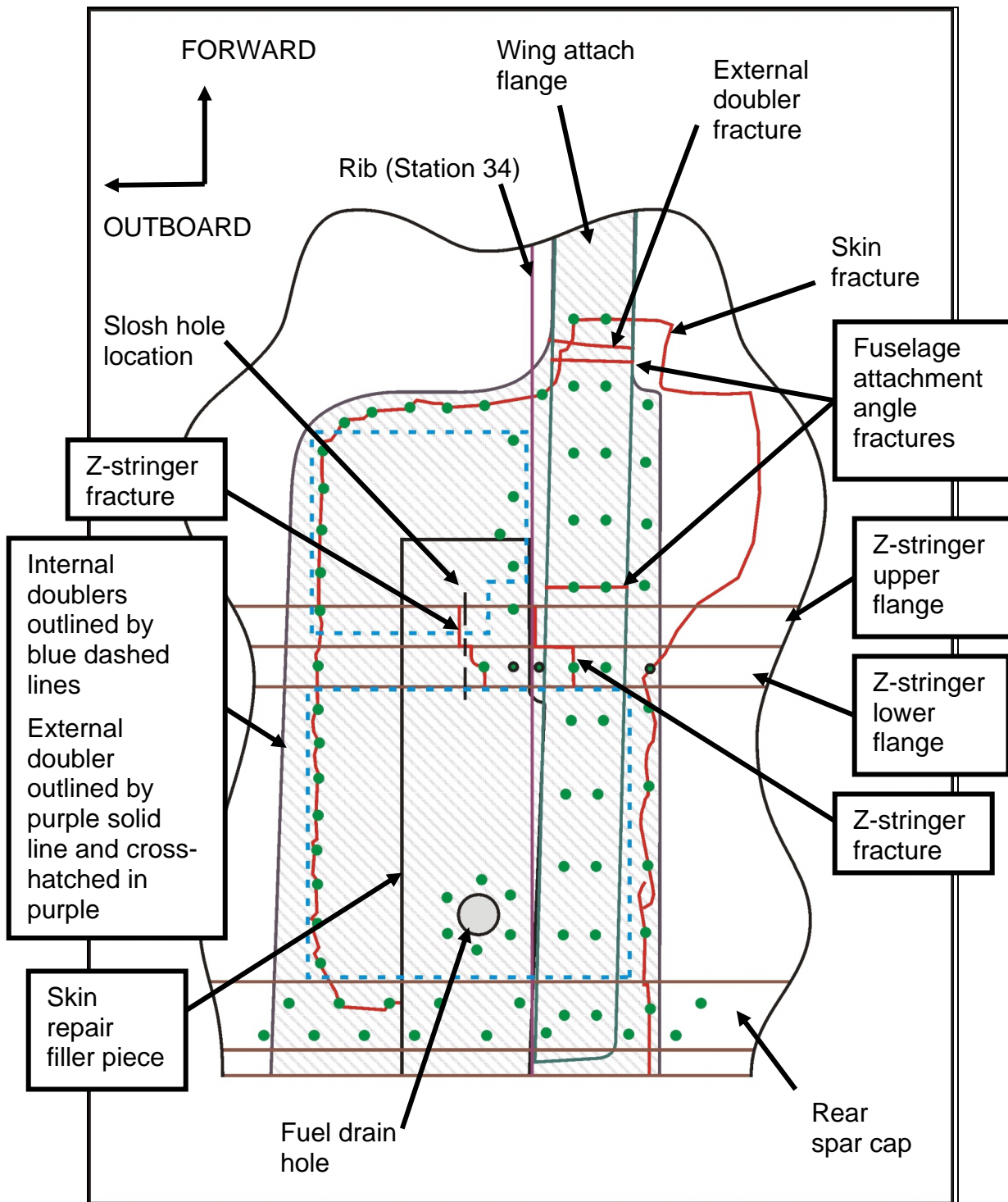


Image No.:0603A00205, Project No.: 2005120013

Figure 38. Schematic view of the wing box beam structure at left WS 34. Selected fastener locations are indicated with solid green circles. Circles with black outlines and green centers indicate holes in the skin and/or stringers that did not have fasteners.



Image No.:0601A00943, Project No.: 2005120013

Figure 39. View of pieces of the wing box beam at left WS 34. The lower skin piece is shown with internal and external doublers removed. The unlabeled arrows and bracket indicate fatigue locations in the skin, Z-stringers, and front spar lower spar cap.

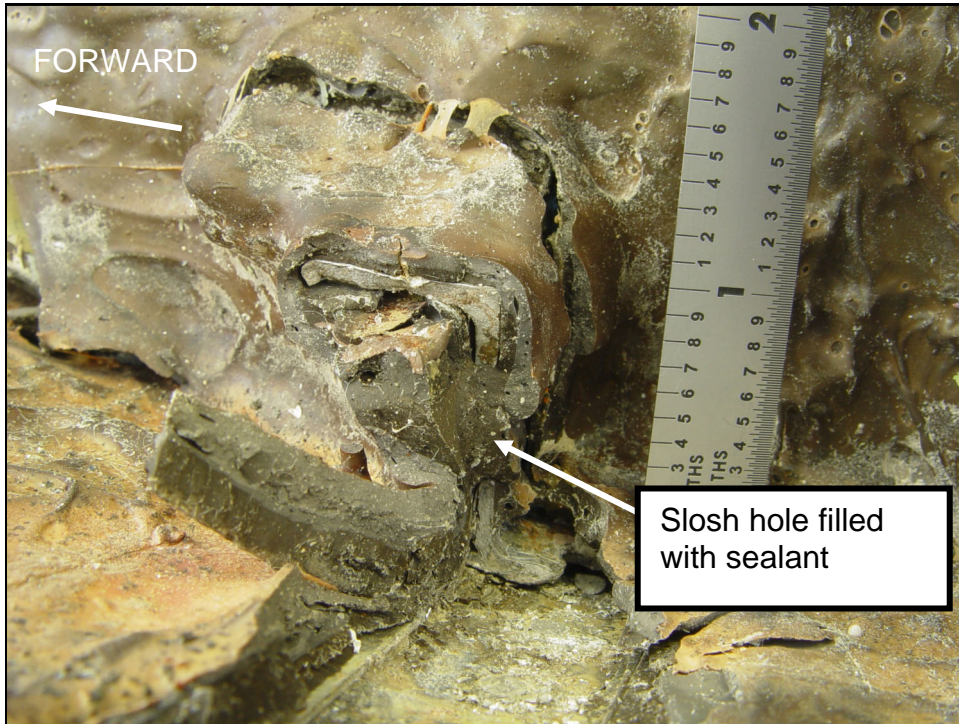


Image No.:0601A00076, Project No.: 2005120013

Figure 40. Close view of the rear Z-stringer fracture just outboard of left WS 34 as received.

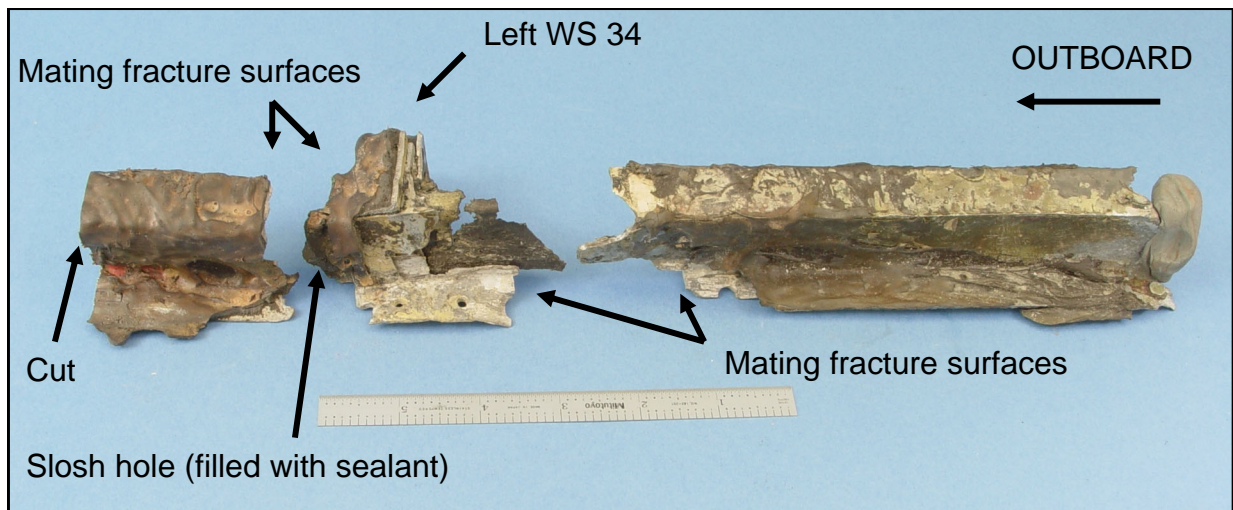


Image No.:0601A01133, Project No.: 2005120013

Figure 41. View of rear Z-stringer pieces from left wing side of the wing box beam lower skin panel shown after separating the piece at left WS 34 from the lower skin and cutting the outboard piece from the rest of a skin panel piece.

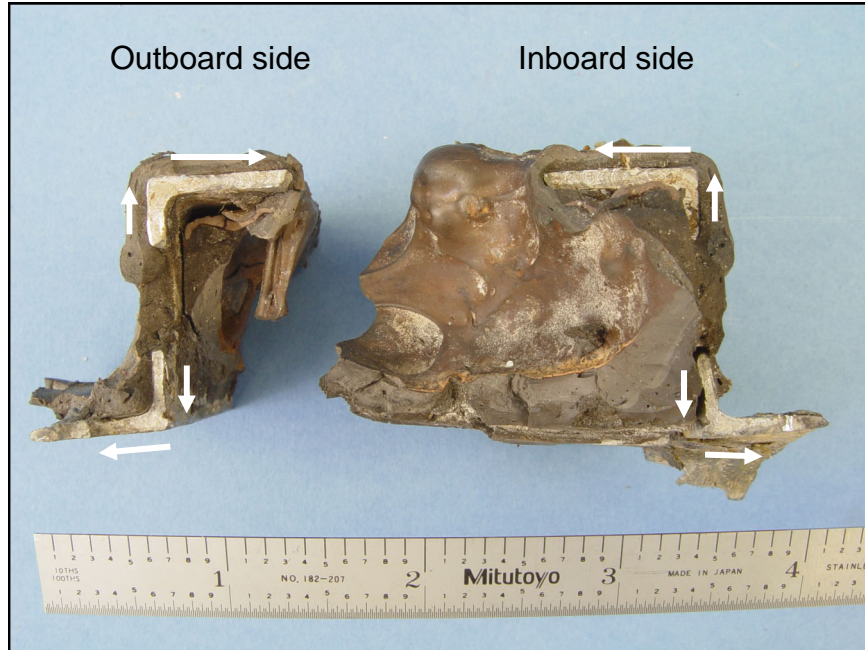


Image No.:0601A01138, Project No.: 2005120013

Figure 42. View of the mating fracture surfaces just outboard of left WS 34 for the rear Z-stringer shown in the previous figure.



Figure 43. Closer view of the outboard fracture surface shown at the left in the previous figure. Unlabeled arrows indicate the directions of fatigue propagation emanating from the slosh hole in the web.

Image No.:0601A01185, Project No.: 2005120013

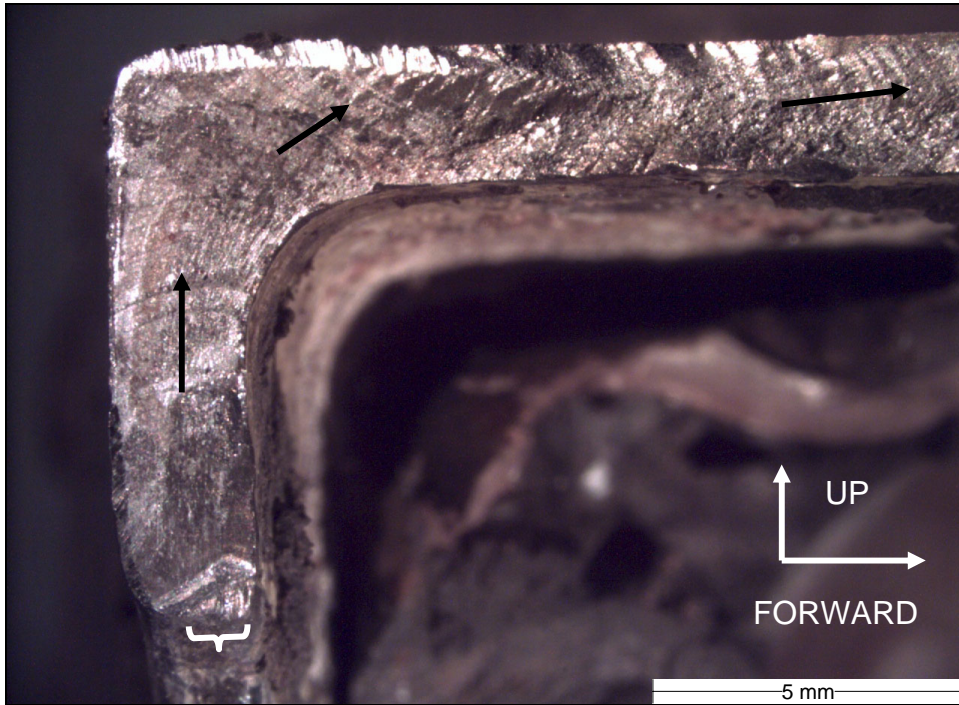


Image No.:0601A01215, Project No.: 2005120013

Figure 44. Close view of fatigue features of the Z-stringer fracture shown in the previous figure at the upper side of the slush hole. Unlabeled arrows indicate general fracture propagation directions and an unlabeled bracket indicates the origin area at the slush hole.

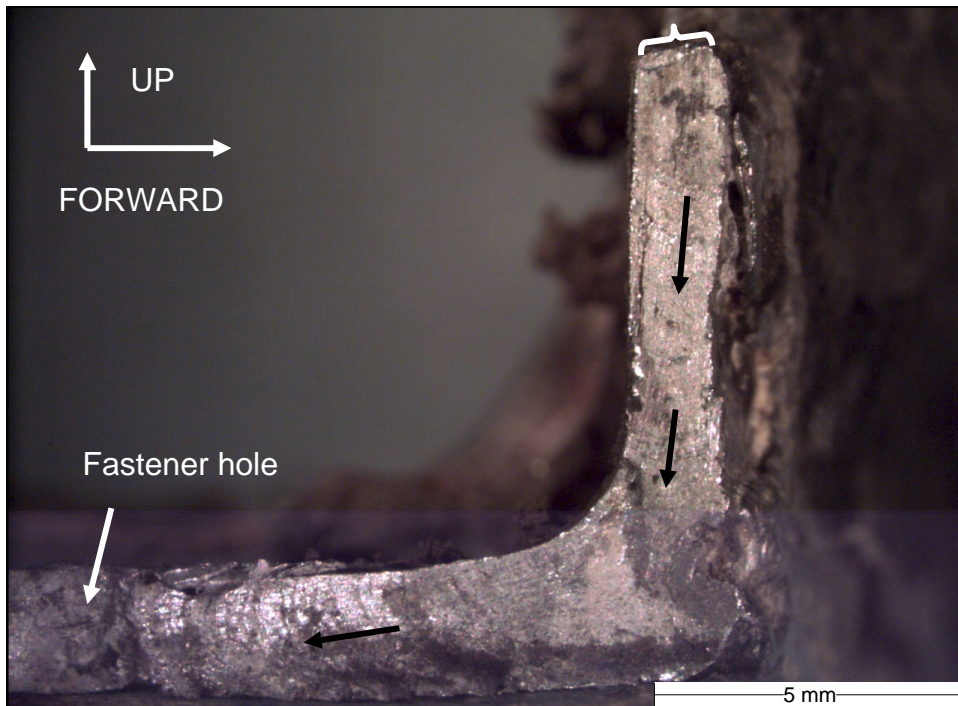


Image No.:0601A01214, Project No.: 2005120013

Figure 45. Close view of fatigue features of the Z-stringer fracture shown in the previous figure at the lower side of the slush hole. Unlabeled arrows indicate general fracture propagation directions and an unlabeled bracket indicates the origin area at the slush hole.

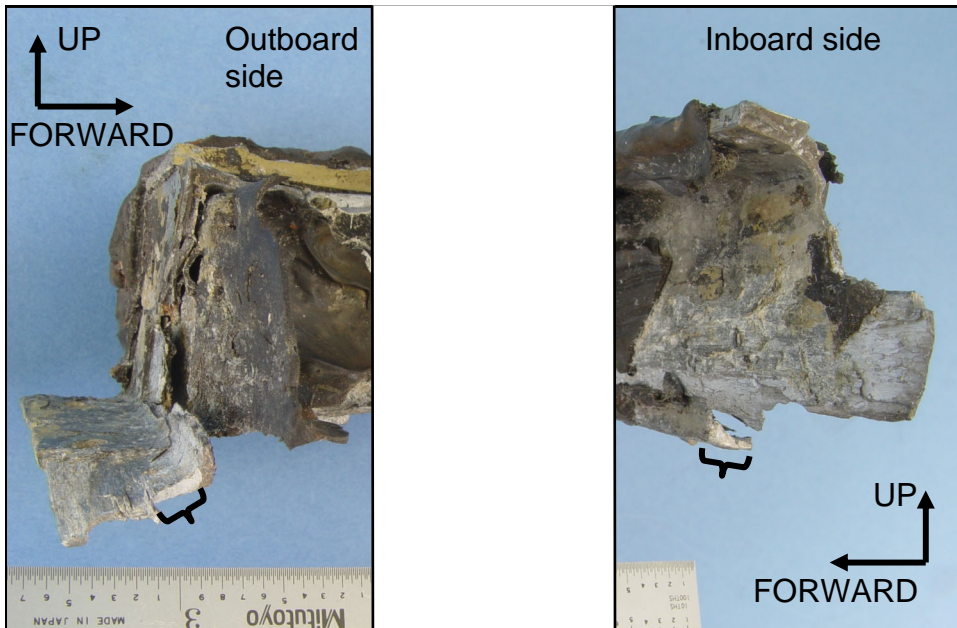


Image No.:0601A01140, Project No.: 2005120013

Figure 46. View of the mating fracture surfaces just inboard of station 34 for the rear Z-stringer shown in figure 41. Unlabeled brackets indicate mating areas of fatigue on the lower flange for the stringer.



Image No.:0601A01141, Project No.: 2005120013

Figure 47. View of the fracture surface for the middle Z-stringer. An unlabeled bracket indicates the extent of a fatigue region emanating from the forward side of a fastener hole, and an unlabeled arrow indicates a small fatigue region at the aft side of the fastener hole.

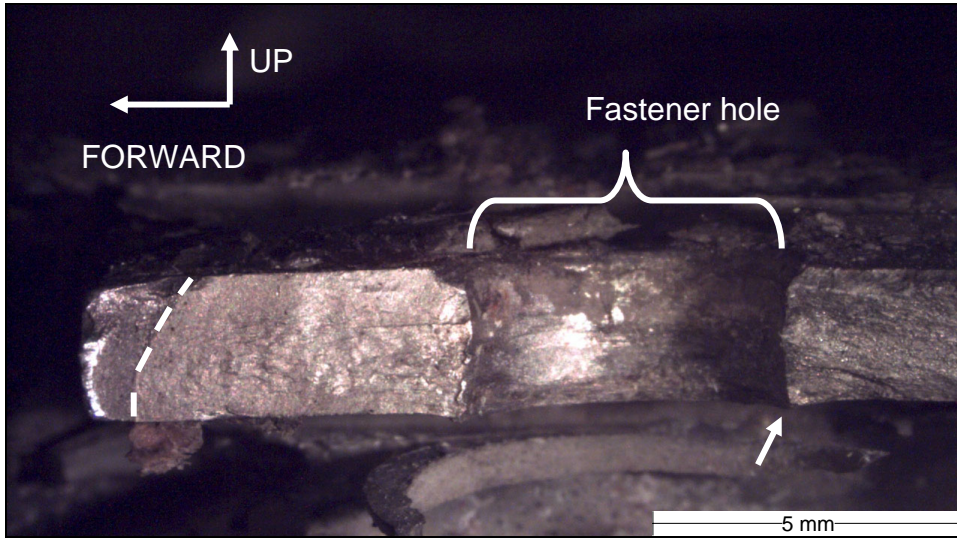


Image No.:0601A01217, Project No.: 2005120013

Figure 48. Close view of the fracture in upper flange of the left wing middle Z-stringer shown in the previous figure. A dashed line indicates the fatigue boundary for the region emanating from the forward side of the fastener hole, and an arrow indicates the smaller fatigue region at the aft side of the fastener hole.

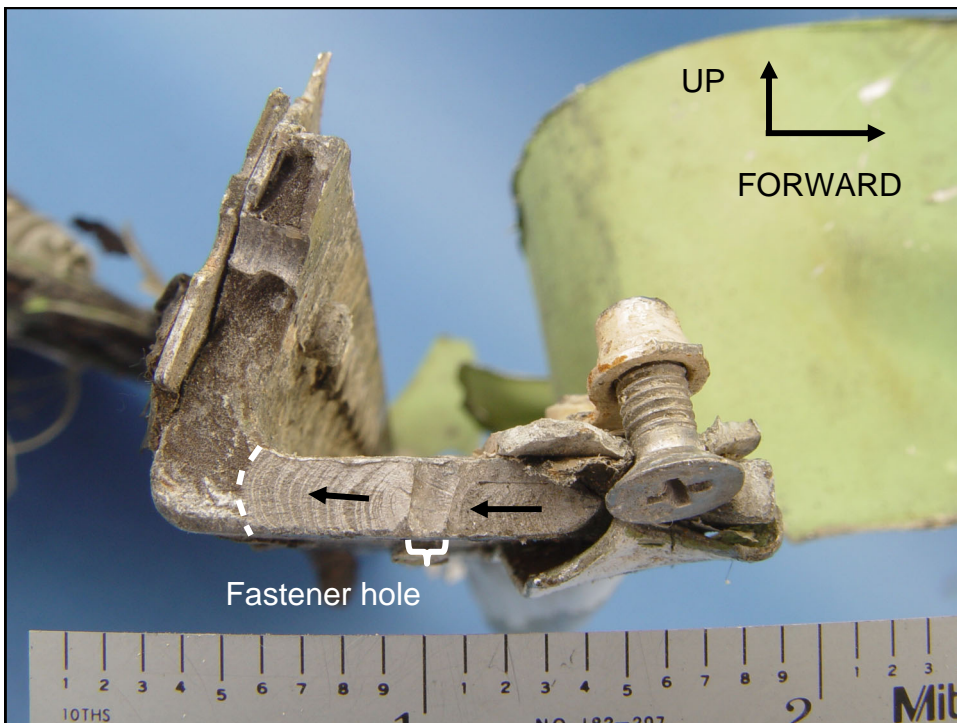


Image No.:0601A01145, Project No.: 2005120013

Figure 49. View of the outboard side of the fracture in the front spar lower spar cap 5 inches outboard of WS 34. A dashed line indicates the fatigue boundary, and unlabeled arrows indicate the direction of fatigue propagation.

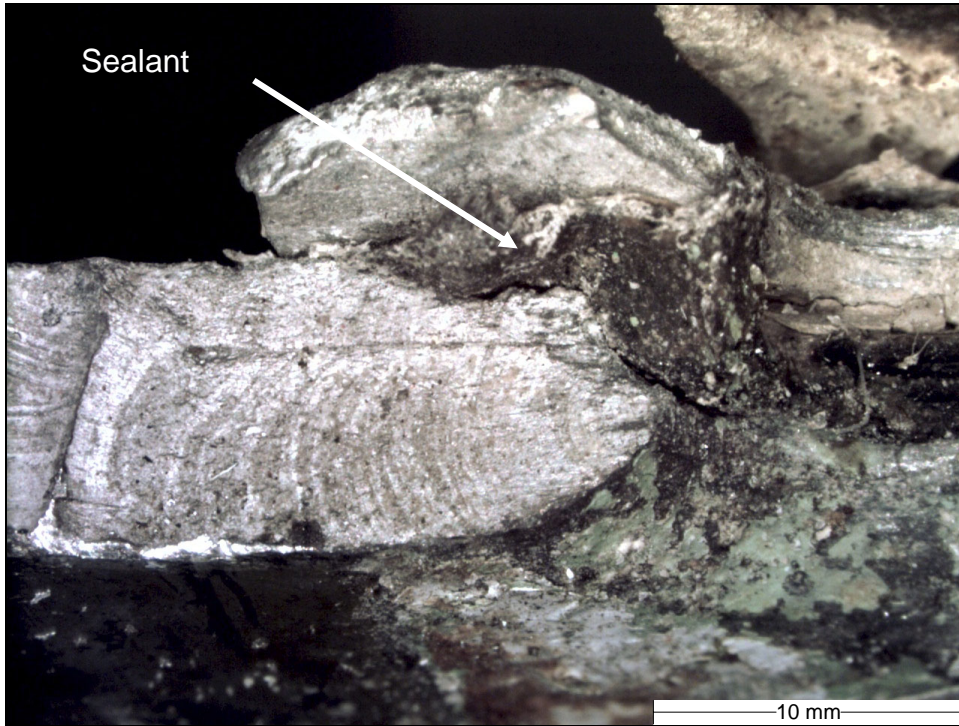


Image No.:0603A01334, Project No.: 2005120013

Figure 50. Closer view of the fatigue origin area in the front spar cap fracture shown in figure 49.



Image No.:0601A01266, Project No.: 2005120013

Figure 51. View of left wing lower skin fracture at inboard fastener holes for doublers. Unlabeled brackets indicate locations where fatigue features emanated from fastener holes.

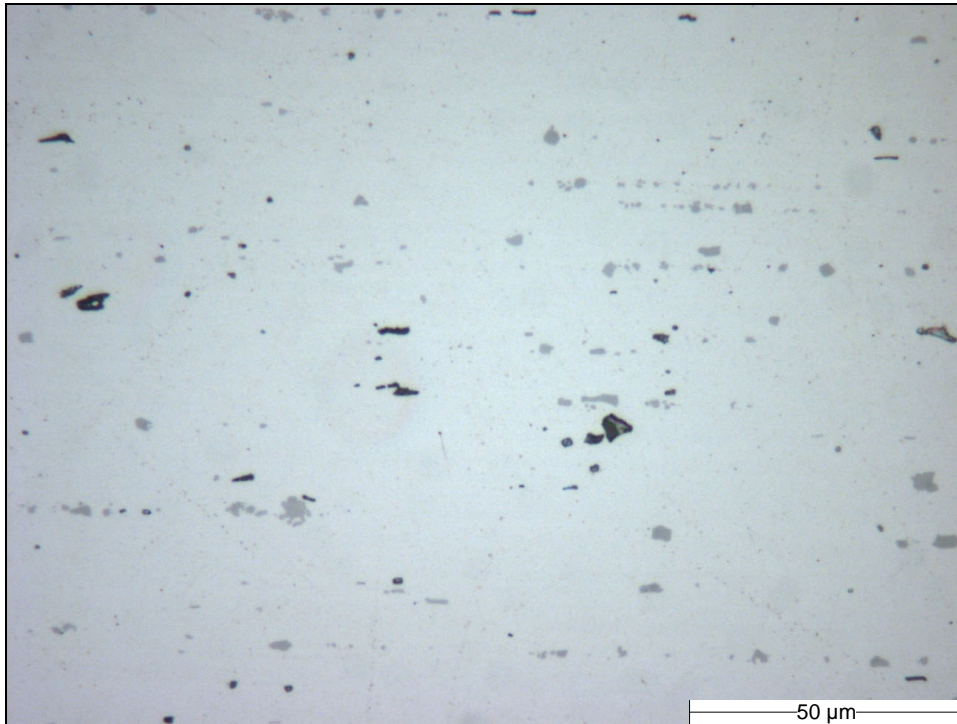


Image No.:0602A00887, Project No.: 2005120013

Figure 52. Rear spar lower spar cap microstructure as polished.

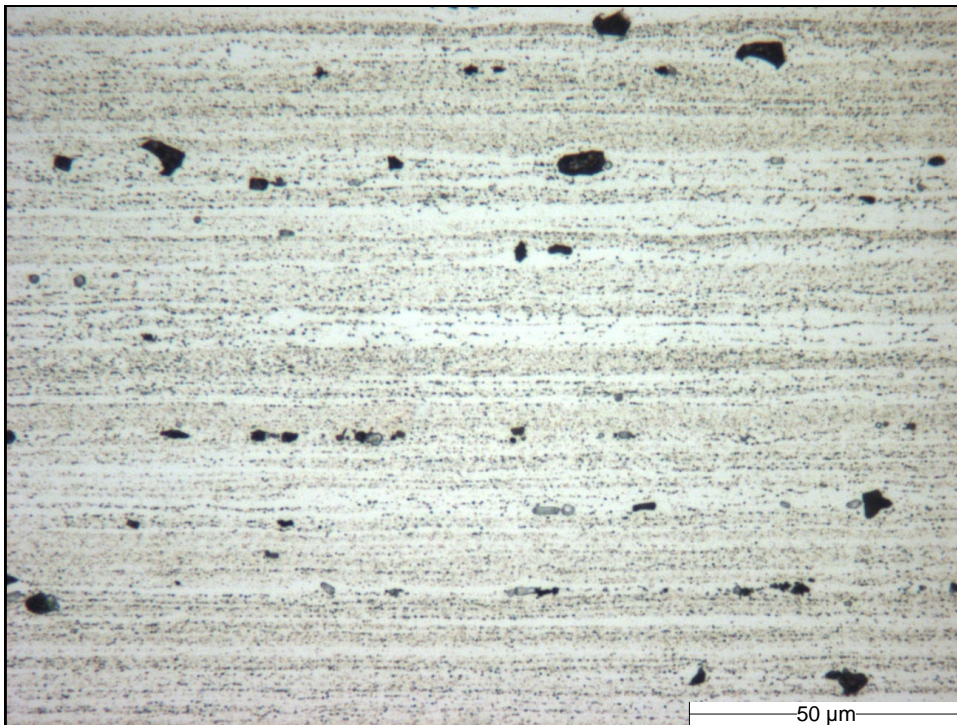


Image No.:0602A00896, Project No.: 2005120013

Figure 53. Rear spar lower spar cap microstructure etched with Keller's reagent.

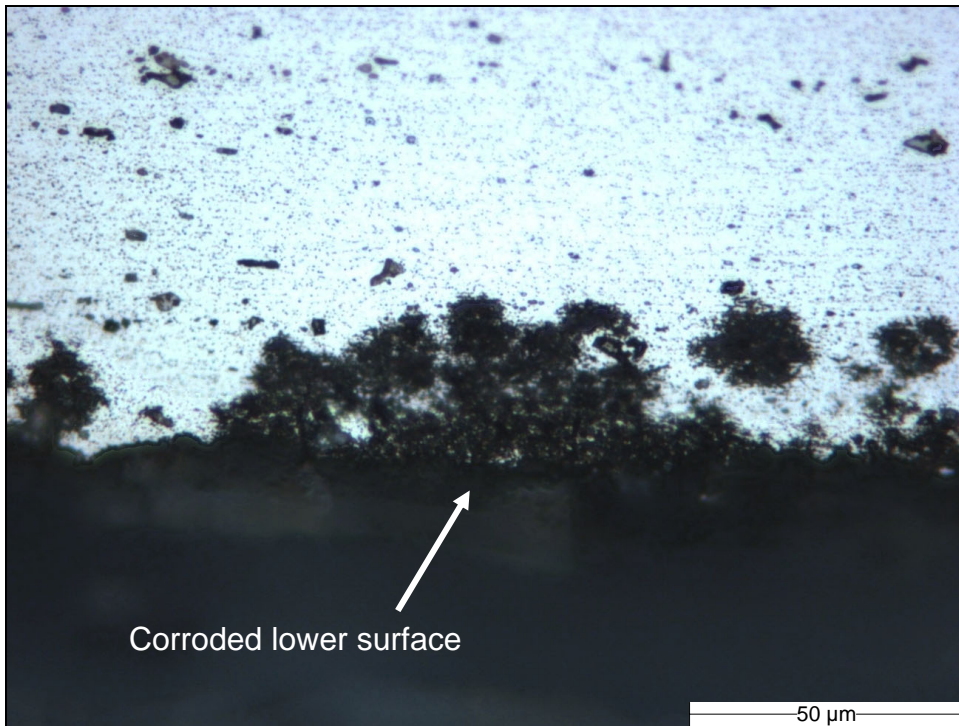


Image No.:0602A00902, Project No.: 2005120013

Figure 54. Rear spar lower spar cap microstructure at the lower surface showing corrosion.

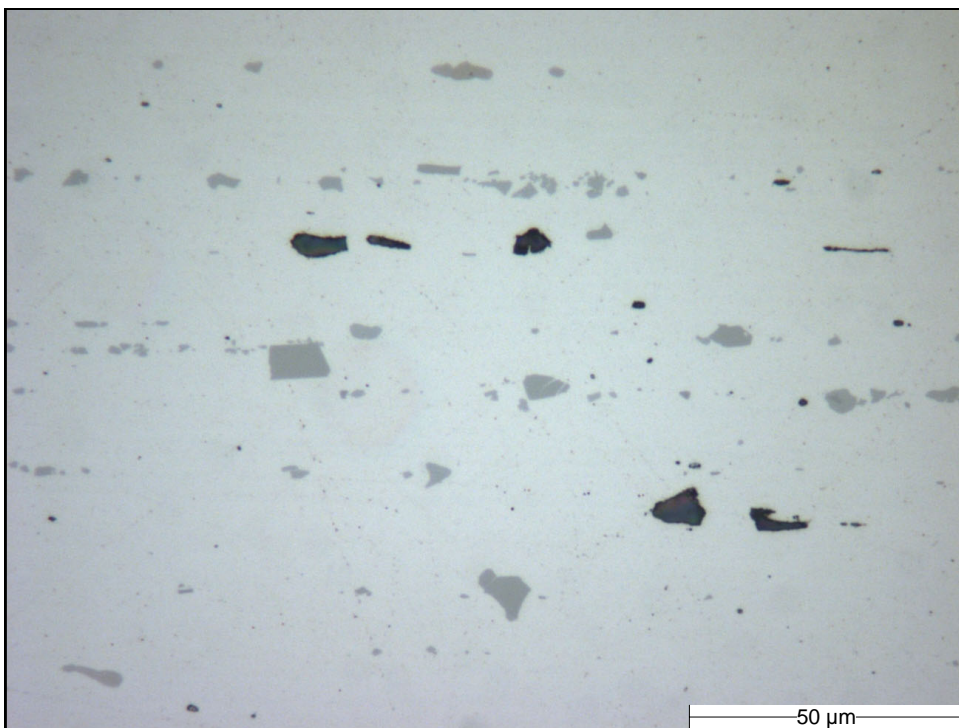


Image No.:0602A00884, Project No.: 2005120013

Figure 55. Rear Z-stringer microstructure as polished.

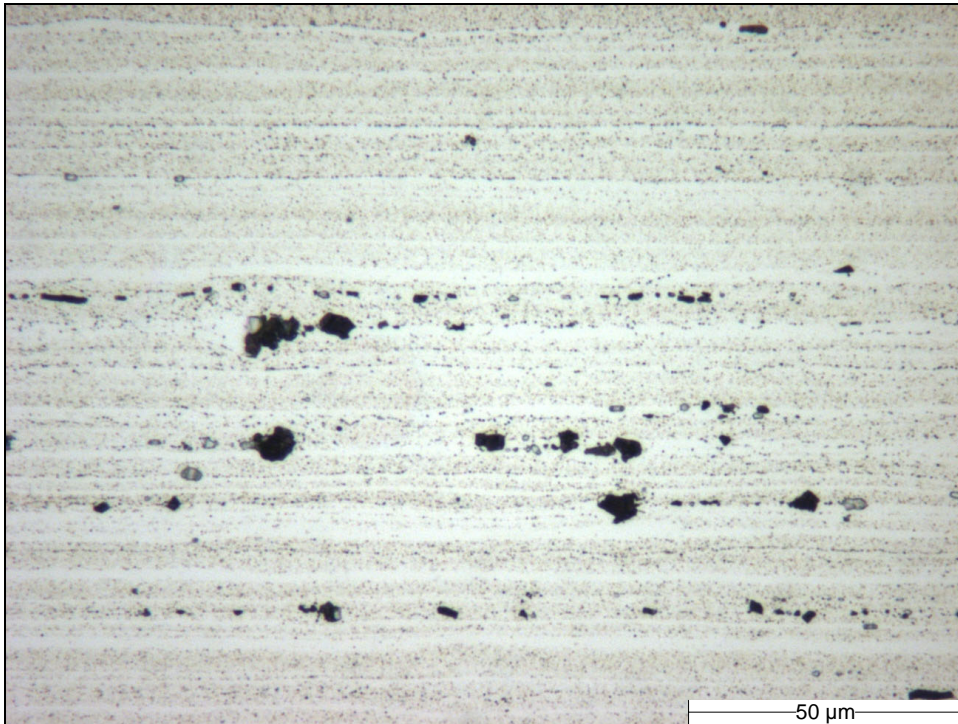


Image No.:0602A00897, Project No.: 2005120013

Figure 56. Rear Z-stringer microstructure etched with Keller's reagent.

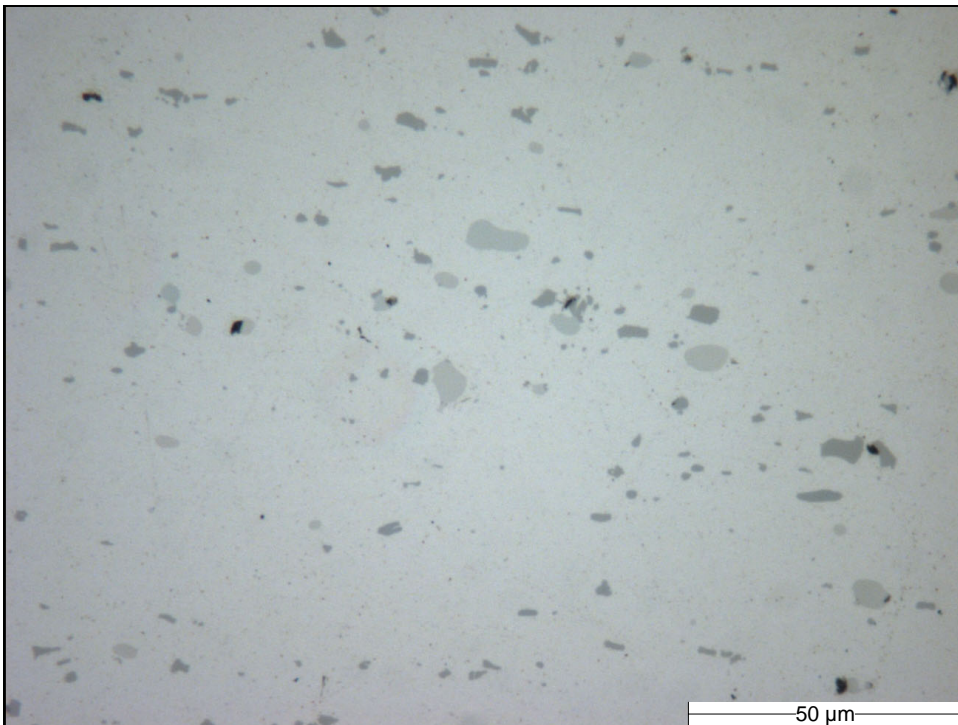


Image No.:0602A00890, Project No.: 2005120013

Figure 57. Lower skin microstructure as polished.

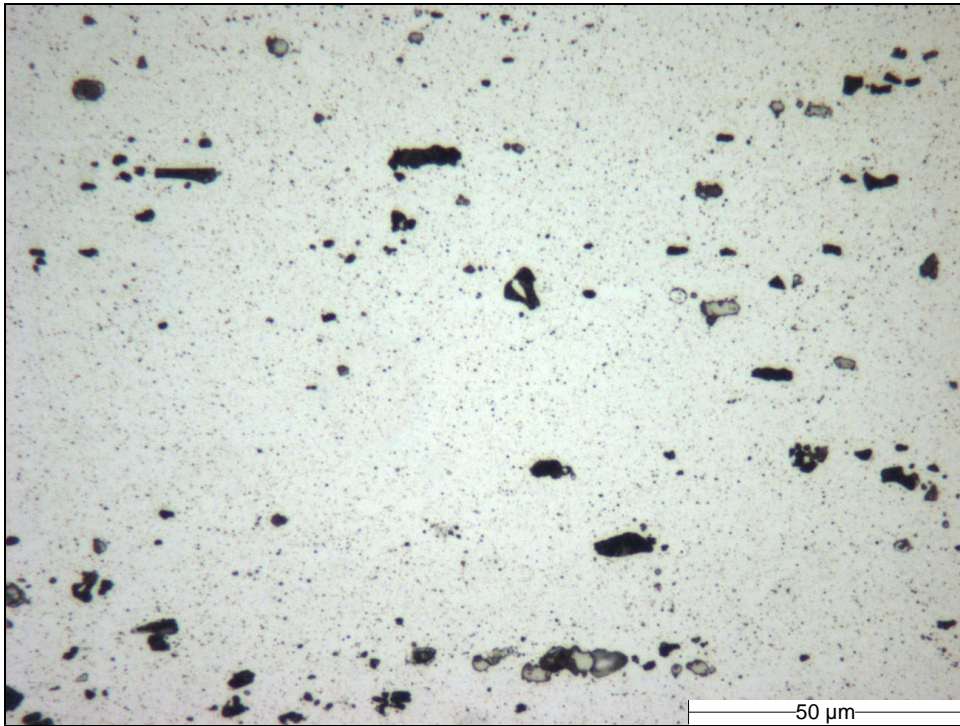


Image No.:0602A00900, Project No.: 2005120013

Figure 58. Lower skin microstructure after etching with Keller's reagent.

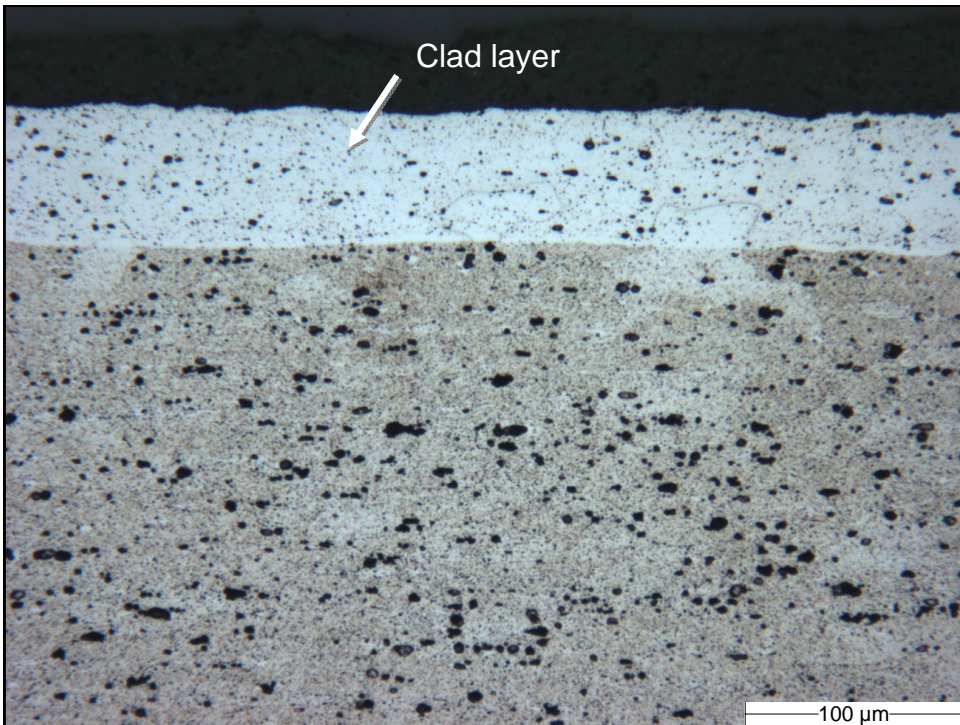


Image No.:0602A00914, Project No.: 2005120013

Figure 59. Lower skin microstructure at the surface after etching with Keller's reagent showing a clad layer.